

# Spatiotemporal variations of air pollutants (O<sub>3</sub>, NO<sub>2</sub>, SO<sub>2</sub>, CO, PM<sub>10</sub>, and VOCs) with land-use types

Jung-Moon Yoo<sup>1</sup>, Myeong-Jae Jeong<sup>2</sup>, Dongchul Kim<sup>3</sup>, William R. Stockwell<sup>4</sup>,  
Jung-Hyun Yang<sup>4</sup>, Hee-Woo Shin<sup>2</sup>, Myoung-In Lee<sup>6</sup>, Chang-Keun Song<sup>7</sup>, and Sang-Deok Lee<sup>7</sup>

<sup>1</sup>Dept. of Science Education, EwhaWomans University, Seoul, Republic of Korea

<sup>2</sup>Dept. of Atmospheric & Environmental Sciences, Gangneung-Wonju National University,  
Gangneung, Gangwon-do, Republic of Korea

<sup>3</sup>Universities Space Research Association, Columbia, MD, USA

<sup>4</sup>Dept. of Chemistry, Howard University, Washington, DC, USA

<sup>5</sup>Dept. of Atmospheric Science and Engineering, EwhaWomans University, Seoul, Republic of Korea

<sup>6</sup>School of Urban & Environmental Engineering, Ulsan National Institute of Science and Technology, Ulsan,  
Republic of Korea

<sup>7</sup>National Institute of Environmental Research, Incheon, Republic of Korea

## ABSTRACT

The spatiotemporal variations of surface air pollutants (O<sub>3</sub>, NO<sub>2</sub>, SO<sub>2</sub>, CO, and PM<sub>10</sub>) with four land-use types: residence (R), commerce (C), industry (I) and greenbelt (G) have been investigated at 283 stations in South Korea during 2002-2013, using routinely observed data. The VOCs data at 9 photochemical pollutant monitoring stations available since 2007 were utilized in order to examine their effect on the ozone chemistry. The land-use types, set by the Korean government, were generally consistent with the satellite-derived land covers and with the previous result showing anti-correlation between O<sub>3</sub> and NO<sub>2</sub> in diverse urban areas. The relationship between the two pollutants in the Seoul Metropolitan Area (SMA) residence land-use areas was substantially different from that outside of the SMA, probably due to the local differences in vehicle emissions. The highest concentrations of air pollutants in the diurnal, weekly, and annual cycles were found in industry for SO<sub>2</sub> and PM<sub>10</sub>, in commerce for NO<sub>2</sub> and CO, and in greenbelt for O<sub>3</sub>. The concentrations of air pollutants, except for O<sub>3</sub>, were generally higher in big cities during weekdays while O<sub>3</sub> showed its peak in suburban areas or small cities during weekends. The weekly cycle and trends of O<sub>3</sub> were significantly out of phase with those of NO<sub>2</sub>, particularly in the residential and commercial areas, suggesting that vehicle emission was a major source in those areas. The ratios of VOCs to NO<sub>2</sub> for each of the land-use types were in the order of I (10.2) > C (8.7) > G (3.9) > R (3.6), suggesting that most areas in South Korea were likely to be VOCs-limited for ozone chemistry. The pollutants (NO<sub>2</sub>, SO<sub>2</sub>, CO, and PM<sub>10</sub>) except for O<sub>3</sub> have decreased most likely due to the effective government control. The total oxidant values (OX = O<sub>3</sub> + NO<sub>2</sub>) with the land-use types were analyzed for the local and regional (or background)

contributions of O<sub>3</sub>, respectively, and the order of OX (ppb) was C (57.4) > R (53.6) > I (50.7) > G (45.4), indicating the greenbelt observation was close to the background.

## 1. Introduction

The spatiotemporal variations in major air pollutants with the land-use types in urban or suburban areas (e.g., Kuttler and Strassburger, 1999; Flemming et al., 2005) are of great interest in densely-populated South Korea because the pollutants from local, regional, and global sources can have an impact on human health and ecosystems (e.g., Cooper et al., 2010; Gilge et al., 2010; Kim et al., 2011; Valks et al., 2011), and on climate change (WMO, 2007). The major surface air pollutants examined in this study were ozone (O<sub>3</sub>), nitrogen dioxide (NO<sub>2</sub>), sulfur dioxide (SO<sub>2</sub>), carbon monoxide (CO), particulate matter (PM<sub>10</sub>) and volatile organic compounds (VOCs). Due to the high energy consumption of South Korea, the country was expected to produce substantial amounts of domestic anthropogenic pollutants (Kim et al., 2013a).

Since air pollutants could be transported from industrialized China to Korea (e.g., Li et al., 2010; Kim et al., 2011; He et al., 2012), their trends and characteristics need to be analyzed in view of international cooperation in reducing the pollutants. The impact of pollutants on a certain area can be associated with its population and emission controls, etc. (Meng et al., 2009). In order to improve the air quality in South Korea, the Ministry of Environment of Korea (MEK) monitored the major pollutants with four land-use types (residence, commerce, industry and greenbelt) set by the Ministry of Land, Infrastructure and Transport (MLIT). Please see Table 1 for the abbreviations in this study. Since the anthropogenic sources of air pollutants, such as transportation and industrial complexes, vary locally with the land-use types, it was more efficient to investigate the spatiotemporal variations of the constituents with the land-use types for our comprehensive analysis and for ultimately controlling them.

Among the major pollutants, CO, nitrogen oxides (NO<sub>x</sub> = NO + NO<sub>2</sub>), PM<sub>10</sub>, and some types of VOCs (e.g., BTEX; benzene, toluene, ethylbenzene, and ortho-, meta-, and para-xylenes) are primarily traffic-induced while O<sub>3</sub> and NO<sub>2</sub> are secondary trace gases formed from precursors in photochemical reactions (e.g., Kuttler and Strussburger, 1999; Masiol et al., 2014). The main sources of SO<sub>2</sub>, the most important precursor for acid rain (Wang and Wang, 1995; Wang et al., 2001), are power plants and heavy industry. The formation of

ground level O<sub>3</sub> also depends on the influx of stratospheric O<sub>3</sub>, the concentrations of NO<sub>x</sub>, NO<sub>y</sub> (i.e., the family of reactive nitrogen species; Pandey Deolal et al., 2012), VOCs, and the ratio of VOCs to NO<sub>x</sub> (Nevers, 2000). When the ratio of VOCs to NO<sub>x</sub> is less than 8 to 10, decreasing NO<sub>x</sub> tends to increase ozone formation (VOC-limited or VOC-sensitive, Larsen et al., 2003; Qin et al., 2004a). On the other hand, when the ratio is higher than 8 to 10, decreasing NO<sub>x</sub> tends to decrease ozone formation (NO<sub>x</sub>-limited or NO<sub>x</sub>-sensitive). However, the value may change due to various factors (e.g., meteorology, deposition, and gas to particle conversion) (Jacobson, 2002).

Nitrogen dioxides have a substantial impact on PM<sub>10</sub> through their atmospheric oxidation to aerosol nitrate, and the CO formed from the oxidation of VOCs (e.g., Wang et al., 2008), and the NO<sub>2</sub> emissions due to most types of anthropogenic combustion are a major O<sub>3</sub> precursor (Gilge et al., 2010; Lamsal et al., 2010, 2011). The SO<sub>2</sub> also leads to photochemical O<sub>3</sub> production with the NO<sub>x</sub> and VOCs under the intense insolation (Klemm et al., 2000; Derwent et al., 2003). In other words, the photochemistry of NO-NO<sub>2</sub>-O<sub>3</sub> system in the tropospheric surface layer is locally controlled by the reactions with CO and many VOCs and even SO<sub>2</sub> (Derwent et al., 2003; Masiol et al., 2014). Meanwhile, the PM<sub>10</sub> aerosol, and the SO<sub>2</sub> and NO<sub>2</sub> gases may act as condensation nuclei or affect the formation of cloud particles in hydrological circulation (Bian et al., 2007). The PM<sub>10</sub> concentrations can affect UV flux and O<sub>3</sub> formation (Qin et al., 2004b; Bian et al., 2007; Han et al., 2011). Therefore, controlling the amount of O<sub>3</sub> is difficult due to non-linear features of its formation reactions (Mazzeo et al., 2005; Jin et al., 2012). In particular, spatiotemporal variations of O<sub>3</sub> in South Korea have not been fully understood yet. Overall, the reactions or interactions of the above pollutants are multiple and complex.

Masiol et al. (2014) reported on the trends and cycles of the pollutants (O<sub>3</sub>, NO<sub>2</sub>, SO<sub>2</sub>, CO, PM<sub>10</sub>, and BTEX) in a large city in northern Italy and they discussed their interactions. There have been dozens of previous studies on the spatiotemporal variations of some substances among the major air pollutants in terms of their cycles (diurnal, weekly and annual) and trends over South Korea. The cycles of each of the pollutants are helpful in order to understand the emission sources, human activities, photochemical processes and meteorological factors that affect it (e.g., Flemming et al., 2005; Meng et al., 2009). Seo et al. (2014) reported that the O<sub>3</sub> trend in South Korea from 1999 to 2010 was similar to that of NO<sub>2</sub> and it increased by +0.26 ppbv yr<sup>-1</sup> possibly due to the local increase in anthropogenic

precursor emissions and meteorological effects. Based on a model simulation, Jin et al. (2012) showed that the Seoul Metropolitan Area (SMA) was VOCs-limited for the O<sub>3</sub> control, while the local province outside the SMA was chemistry between VOCs-limited and NO<sub>x</sub>-limited. However, Kim et al. (2013b) reported that in the suburban SMA, the biogenic VOCs could be the most important source of high O<sub>3</sub> episodes. The temporal O<sub>3</sub> averages in the SMA and other inland areas were low as a result of an increase in O<sub>3</sub> titration by NO from enhanced NO<sub>x</sub> levels compared to those at the coastal areas sometimes due to a land-sea breeze (Ghim and Chang, 2000; Oh et al., 2006; Seo et al., 2014). In other words, the titration can slow down the O<sub>3</sub> accumulation in the urban (or suburban) areas due to significant concentrations of NO (Chou et al., 2006).

The long-term NO<sub>2</sub> trends in South Korea from 1998 to 2008 were different between Seoul and other cities with more declining trends at the Seoul sites (Shon and Kim, 2011), presumably due to the MEK effort to reduce the NO<sub>x</sub> emissions from the SMA (Kim et al., 2013a). Diurnal and seasonal variations in the individual VOCs at a site in Seoul in 2004 were measured by Nguyen et al. (2009), provided information on the relative abundance of anthropogenic emissions compared to natural emissions. Long-term changes in the PM<sub>10</sub> in South Korea in some periods between 1992 and 2010 were reported in urban areas by Kim and Shon (2011), and Sharma et al. (2014), and at the background site of Gosan by Kim et al. (2011). Meanwhile, Flemming et al. (2005) investigated the cycles of the four air pollutants (O<sub>3</sub>, NO<sub>2</sub>, SO<sub>2</sub>, and PM<sub>10</sub>) in Germany based on an objective air quality classification scheme of hierarchical clustering.

The weekend effect, derived from the weekly cycle, has been focused primarily on the relationship between O<sub>3</sub> and NO<sub>2</sub> in many previous studies (e.g., Brönnimann et al., 2000; Fujita et al., 2003a, 2003b; Beirle et al., 2003; Qin et al., 2004b). In these studies, they examined the weekend effect because it can be an indicator of urbanization or human activity (Atkinson-Palombo et al., 2006). For instance, the analysis of the NO<sub>x</sub> weekly cycle could be useful in discriminating between its anthropogenic (e.g., local traffic) and natural sources (Beirle et al., 2003). The weekly cycles (or weekend/weekday effect) of O<sub>3</sub>, NO<sub>x</sub>, and VOCs provide insight into NO<sub>x</sub> and VOCs limitation as well. Particularly, the analysis with the land-use types in our study can be helpful in estimating various kinds of man-made emissions (e.g., vehicles and factories, etc). Despite relatively low concentrations of O<sub>3</sub> precursors (NO<sub>x</sub> and VOCs) during the weekend, 'high O<sub>3</sub> concentrations' at that time were observed in

California (Marr and Harley, 2002a, 2002b; Qin et al., 2004b), in remote areas (Brönnimann et al., 2000; Pudasainee et al., 2006), and in Japan (Sakamoto et al., 2005). In more detail, Beirle et al. (2003) examined the weekly cycle of the tropospheric NO<sub>2</sub> Vertical Column Densities (VCD) emitted by anthropogenic sources from a number of metropolises throughout the world, using satellite data from the Global Ozone Monitoring Experiment (GOME) during the 1996-2001 period. According to their report, NO<sub>2</sub> concentration tended to decrease on weekends when human activity was relatively low. Qin et al. (2004b) revealed that in southern California, the VOCs sensitivity at weekend, accompanied with the reduced NO<sub>x</sub> and PM<sub>10</sub> emissions, could result in enhanced O<sub>3</sub> formation, although this tendency was not shown in some areas close to the beach and far downstream from L.A. downtown. This result suggests that the weekend effect may vary with meteorological factors (e.g., Jacobson, 2002) and land-use types. A study on their reactive relationship (O<sub>3</sub>, NO<sub>2</sub>, and VOCs) with the land-use types in South Korea is required in order to explain the possible causes for the O<sub>3</sub> formation and to make a policy decision for either NO<sub>x</sub>-limited or VOCs-limited regimes for the formation over the country.

As we mentioned earlier, the spatiotemporal analyses of some species among the major air pollutants have been assessed in many previous studies in terms of their cycles, trends, and interactions, although the VOCs analyses are still lacking due to the limited observations and data. To the best of our knowledge, there have not been any comprehensive studies on the spatiotemporal variation of the major air pollutants at 283 stations over South Korea associated with land-use types, using simultaneous measurement data from a dense observational network. The VOC data available since 2007 have also been utilized to examine the relative influences of VOCs and NO<sub>2</sub> on the O<sub>3</sub> change. A large number of data on the 0.1° × 0.1° or 0.25° × 0.25° spatial grids were developed to better understand the spatiotemporal variations of the pollutants with the types requires high quality, long-term observations of these reactive substances.

The purpose of this study was to comprehensively investigate the spatiotemporal variations and their consistency of the major pollutants over the four land-use types in terms of their cycles, trends, and relationships, based on simultaneous hourly observations at the stations located in urban or suburban areas in South Korea. In section 2, we briefly describe the data and measurements of the pollutants. In addition, we introduce the indices of the land surface properties derived from the satellite data to compare the four land-use types of the

MEK. In section 3, we describe the air pollutant data on the two spatial grids:  $0.1^{\circ} \times 0.1^{\circ}$  and  $0.25^{\circ} \times 0.25^{\circ}$  with the characteristics of the gridded land-use type data. In section 4, the climatological pollutant averages are given for the seasons and the land-use types, respectively. The results for their cycles and trends are described in sections 5 and 6, respectively. We investigate the relationship between  $O_3$  and  $NO_2$  with the land-use types and discuss the results in section 7, and the weekend effect ( $O_3$ ,  $NO_2$  and VOCs) in section 8. Finally, the conclusions are provided in section 9.

## 2. Data and Method

The information for the surface air pollutants ( $O_3$ , CO,  $NO_2$ ,  $SO_2$ ,  $PM_{10}$  and VOCs) data used in this study is presented in Table 2. Hereinafter the four pollutants (CO,  $NO_2$ ,  $SO_2$ , and  $PM_{10}$ ) will be called ‘the CNSP pollutants’ in this study. The above pollutants except VOCs have been measured each hour at 283 air pollution monitoring stations of the MEK in South Korea during the period from January 2002 to December 2013 (Figs. 1a-d), while the VOCs data at 19 stations were available since 2007. The majority of observational sites were located in urban or suburban areas rather than remote areas. These pollutants were predominantly produced by mobile and stationary combustion, and/or photochemical processes (Masiol et al., 2014). Nine out of the 19 VOCs stations were selected in this study based on the criteria of better co-location of the observational sites and longer data records since 2007 (Table 2 and Fig. 1e). The VOCs at the 9 MEK photochemical stations were simultaneously observed with the other pollutants at the same sites. Figure 1f shows the locations of seven major cities in South Korea with the background map, based on the satellite-derived AVHRR land-cover types.

In order to enhance the efficiency of land-use, the MLIT classified the land of South Korea into the four land-use types as follows: 154 residential (R), 57 commercial (C), 35 industrial (I) and 37 greenbelt (G) stations (See Tables 1-2 for details). According to Article 36 of the National Land Planning and Utilization Act ([http://www.law.go.kr/engLsSc.do?menuId=0&subMenu=5&query=NATIONAL\\_LAND\\_PLANNING\\_AND\\_UTILIZATION\\_ACT#liBgcolor2](http://www.law.go.kr/engLsSc.do?menuId=0&subMenu=5&query=NATIONAL_LAND_PLANNING_AND_UTILIZATION_ACT#liBgcolor2)), urban or suburban areas are designated. The areas of the four land-use types have been subdivided based on Article 30 of the Enforcement Decree of the National Land Planning and Utilization Act (Please see the

above link at <http://www.law.go.kr/>, keyword: National Land Planning and Utilization Act). In addition the MLIT criteria for the types are available in the supplementary data in Korean (<http://www.law.go.kr/>, keyword: National Land Planning and Utilization Act in Korean).

The hourly observations of the pollutants, except for the VOCs, during the 12 year period were utilized for the temporal cycle and trend analyses over the land-use types. The hourly data were arranged into 144 monthly anomaly values in order to remove the annual cycle in the time series. The anomaly value was computed by subtracting the climatology (i.e., 12 year monthly mean in this study) from the monthly average in a given month. The 95% confidence intervals for the trends were calculated using the bootstrap method (Wilks, 1995). For each air pollutant anomaly data set, 10,000 new data sets were created to produce 10,000 linear trends through random sampling (e.g., Lee et al., 2013). The random sampling was conducted by drawing data out of the respective original records of the air pollutant anomalies, allowing repetition. The  $\pm$  values in the trend analysis defined the 95% confidence intervals, while they stood for  $1\sigma$  (standard deviation) in the concentration averages.

The details of the surface air pollutants measurements including the instrumentation and methods are given in Table 3. The O<sub>3</sub> concentrations were measured by a Thermo 49i analyzers using the ultraviolet (UV) photometric method (e.g., Diaz-de-Quijano et al., 2009). The non-dispersive infrared method was utilized to measure the CO with a Thermo, 48CTL. The NO<sub>2</sub> was measured by a Thermo, 42CTL using the chemiluminescence method. The Thermo, 43CTL was used to measure the SO<sub>2</sub>, based on the pulsed UV fluorescence method. The PM<sub>10</sub> was measured by a Thermo, Model FH62-C14 (<http://www.thermo.com>) with the  $\beta$ -ray absorption method (e.g., Elbir et al., 2011). The control methods, which avoided high humidity in the measurement systems, were discussed in detail in Yoo et al. (2014).

For the VOC observations, the water vapor in the air samples, which were collected every hour, was removed from the air using a Nafion Dryer. A total of 56 VOC species were identified and quantified using a combination of the on-line thermal desorption system (Unity/Air Server, Markes) and the GC/Deans switch/Dual FID system (Varian 3800 GC, USA). These VOC compounds could be grouped into alkyne (1), aromatic (16), olefin (10), and paraffin (29) groups (Nguyen et al., 2009). The quality check for the GC was carefully calibrated, which was routinely conducted by site managers.

Uncertainty of the measurement instruments for each pollutant is available in NIER (2010). According to the NIER's report, the minimum requirements of the measuring

instruments for accuracy (or uncertainty) are ‘less than 0.005 ppm’ for O<sub>3</sub>, NO<sub>2</sub>, and SO<sub>2</sub>, ‘less than 0.5 ppm’ for CO, and ‘less than 2 % of measuring range’ for PM<sub>10</sub>. Also the uncertainty for VOCs is within ±20 % of true value. The uncertainties for the CO and SO<sub>2</sub> with respect to their typical values are relatively large compared to other pollutants (O<sub>3</sub>, NO<sub>2</sub>, PM<sub>10</sub>, and VOCs).

In order to approximately examine the validity of the four MEK land-use types at 283 sites in South Korea, we compared them with satellite derived land-covers of both the AVHRR and MODIS in a 0.25° x 0.25° grid (Table 4). The AVHRR data were provided for 13 land covers over the globe at a 1 km x 1 km pixel resolution, time-averaged during 1981-1994 (e.g., De Fries et al., 1998; Hansen et al., 2000). The MODIS data were derived for 17 land covers over the globe at a 5 km x 5 km spatial resolution from 2002 to 2012 (e.g., Friedl et al., 2010), and they were available each year.

Although the land covers of both of the satellites were obtained from different periods, the AVHRR and MODIS original types were regrouped in this study and compared for the following four land covers: forest/woods, grass/shrub, urban/built-up, and water (Table 4). The MODIS ‘water’ covers with the land-use types were not changed during the year period, and the covers were greater in the MEK ‘industry and greenbelt’ types than in the ‘commerce and residence’ types (Fig. 3d). In Table 4, the values with and without parentheses indicate the MODIS and AVHRR data, respectively. The MEK land-use types, set by the Korean government, were generally consistent with the satellite-derived land covers. The MEK ‘greenbelt’ type compared to the three other types highly corresponded to the satellite-derived ‘forest/wood’ (35.2-37.2 %) cover, but rarely to the ‘urban/build-up’ (0-16.4 %). For AVHRR, the ‘water’ like river dominated in the MEK types of ‘greenbelt’ and ‘industry’, while the ‘urban and built’ matched well with the MEK ‘commerce’ type (Fig. 2). The ‘industry’ areas were expected to be located near rivers for transportation.

Figure 3 shows the interannual variations in the MODIS-derived land-cover types (%) versus the MEK four land-use types from 2002 to 2012. The interannual variations in the MODIS land-cover with respect to the MEK types were not significant during that time period. It is reasonable that MODIS ‘forest/wood’ covers were the greatest (37.2%) in the MEK ‘greenbelt’ type (Fig. 3a and Table 4). In the MEK ‘residence’ type, the MODIS ‘forest/wood’ cover was slightly increased, but the ‘grass/shrub’ cover had decreased (Fig. 3a-b). The MODIS ‘urban/build-up’ was at a minimum (16.4%) in the MEK ‘greenbelt’ and



at a maximum (32.2%) in the ‘commerce’ (Fig. 3c and Table 4). In addition, the validity of the MEK types was investigated again in section 7 of this study in terms of the relationship between O<sub>3</sub> and NO<sub>2</sub>. The inverse relationship between the two variables over the various land-use types of urban areas has been studied significantly in previous studies (e.g., Kuttler and Strassburger, 1999, their Fig. 3; <http://www.sciencetime.org/ConstructedClimates/chap-4-emissions-urban-air/3-9-complicated-ozone>; Masiol et al., 2014, their Fig. 5).

### **3. Air pollutant data on the two spatial grids: 0.1°×0.1° and 0.25°×0.25°**

In this study we rearranged the non-gridded pollutant data on the two spatial grids (0.1°×0.1° and 0.25°×0.25°) to examine urban characteristics of the gridded land-use type data due to the non-uniform distribution of the pollution monitoring stations. The pollutants, except for VOCs, were investigated as time-averaged in the two spatial grids after categorizing the 283 station data in the four land-use types. The stations are mostly located in the urban areas with a very sparse distribution in the rural areas (Fig. 1). The higher spatial resolution of the 0.1°×0.1° grid generally tends to represent the characteristics of large urban cities better than in suburban regions, when they were compared to those of coarser resolution (i.e., 0.25°×0.25°). For example, the more urbanized stations over the SMA contribute more to the number of the high resolution grid than that of the low resolution grid. In other words, since the number of stations are larger in the big cities (i.e., more urban features) than in the small cities (i.e., fewer urban features), the higher resolution grid displays more in the former cities than in the latter. Although this tendency is also shown in the lower resolution grids, the weighting effect of the big city characteristics is more substantial in the 0.1°×0.1° grid than in the 0.25°×0.25° grid.

Because of the difference in the numbers of stations in each grid, the grid numbers that returned the valid grid-averages of observations at the 0.1°×0.1° and 0.25°×0.25° resolutions with respect to the non-gridded 283 stations were reduced to 196 (R; 89, C; 42, I; 32, G; 33) for the 0.1°×0.1° and 146 (R; 59, C; 30, I; 25, G; 32) for the 0.25°×0.25° resolutions, respectively. Different land-use type data (e.g., two residential and three greenbelt stations) can coexist in a given grid. In this case, the pollution data in the grid have been utilized for the arithmetic average calculation for the residential and greenbelt types, respectively.

The choice of either  $0.1^\circ \times 0.1^\circ$  or  $0.25^\circ \times 0.25^\circ$  grid boxes as an optimal spatial grid scale represents a compromise based on keeping the intrinsic spatial variability of the pollutants ( $O_3$ , CO,  $NO_2$ ,  $SO_2$  and  $PM_{10}$ ) of interest, namely their concentrations, at comparable levels and still having large enough total sample size, i.e. the number of grid boxes with pollutant data, for a robust computation. The variability has been examined in terms of some dimensionless measure (i.e., the ratio of standard deviation ( $\sigma$ ) to mean ( $\bar{X}$ ); Yoo et al., 2014) in the climatological annual average distribution of the pollutants. The  $\sigma/\bar{X}$  values for the five air pollutants at the two different types of grids range from 15.0 % to 45.0 %. Since the  $\sigma/\bar{X}$  values at a  $0.1^\circ \times 0.1^\circ$  grid are 16.3-44.0 %, they are within the range (15.0-44.9 %) at a  $0.25^\circ \times 0.25^\circ$  grid.

#### **4. Climatological seasonal distributions of the pollutants: $O_3$ , CO, $SO_2$ , $NO_2$ and $PM_{10}$**

Figure 4 shows the spatial distributions of the climatological seasonal averages of  $O_3$  (ppb), CO (0.1 ppm),  $NO_2$  (ppb),  $SO_2$  (ppb) and  $PM_{10}$  ( $\mu\text{g m}^{-3}$ ) in a  $0.25^\circ \times 0.25^\circ$  grid over South Korea from 2002 to 2013. The seasonal and annual averages of the five pollutants are summarized in two different types of spatial grids ( $0.25^\circ \times 0.25^\circ$  and  $0.1^\circ \times 0.1^\circ$ ) in Table 5. In the table, the standard deviation ( $\sigma$ ) values of the five pollutants are also presented with the  $\pm$  values. The distributions were highly seasonal. The peak season of  $O_3$  in South Korea was in the spring (March, April and May) than in the summer (June, July and August) due to the summertime monsoon and clouds. The  $O_3$  level was the lowest in the winter due to the low photolysis (Table 5). Higher concentrations of the CNSP pollutants appeared in large cities (e.g., the SMA) more often than in suburban/rural areas. However, the  $O_3$  values were lower over the large cities than over either their outer or coastal regions due to its reaction with other air pollutants and meteorological conditions (Seo et al., 2014). According to their study, the  $O_3$  values over the large cities were low because of the NO titration even during the night without photochemical reactions by local anthropogenic precursor emissions, while they were high in the coastal areas because of the sea breeze effect. Since  $O_3$  and NO do not coexist at night, NO tends to be efficiently transformed into  $NO_2$  (Mazzeo et al., 2005). The higher  $O_3$  level in the rural areas throughout the seasons indicated the role of oxidization during the transport. Flemming et al. (2005) also reported that the high  $O_3$  levels in the rural area could be linked to the low level of NO emissions (e.g., the VOCs role; Ahrens, 2007). It is noted

that seasonal O<sub>3</sub> concentrations in Jeju island (Jeju station; 33.51N, 126.53S) were higher than those found inland while the opposite situations were found for the other pollutants.

The seasonal CNSP pollutant concentrations were lower in summer due to heavy rainfall (despite high but intermittent photolysis rates) than in winter, when O<sub>3</sub> value was the lowest (Fig. 4 and Table 5). The maximum values of the CO, NO<sub>2</sub> and SO<sub>2</sub> were shown in the winter due to the low boundary layer height (e.g., Kaiser et al., 2007) followed by the spring and the fall (see also Fig. 6c discussed later). Higher values of CO, NO<sub>2</sub> and PM<sub>10</sub> over the SMA than in other regions were explained by the large population density and traffic emission, and industrial activity (Fig. 4). Higher NO<sub>2</sub> values in the SMA were also reported by Seo et al. (2014). The high SO<sub>2</sub> values over the coastal regions were due to the factories and power plants, and the high CO values inland were due to the active fossil fuel burning. Asian dust aerosol (e.g., PM<sub>10</sub>) transported from China contributed to the spring peak in PM<sub>10</sub>, and its spring maximum was due to lower amounts of precipitation than in other seasons (Table 5). These results suggest that the meteorological conditions were an important factor characterizing the seasonality of the air pollutants, while the emissions determined the magnitudes of the pollutants.

The amounts of CNSP pollutants were larger in a 0.1°×0.1° grid, while the O<sub>3</sub> values were larger in a 0.25°×0.25° grid (Table 5). In particular, the annual value for NO<sub>2</sub> was remarkably greater by 16% in the former than in the latter, suggesting that the vehicle emissions in the urban area were a primary source for that pollutant. On the other hand, the annual value for O<sub>3</sub> was smaller by 6% in the 0.1°×0.1° grid than in the 0.25°×0.25° grid, implying that the O<sub>3</sub> levels in the suburban/rural/coastal areas were higher than in the urban ones (Fig. 4). These features were clear in the seasonal and annual values (Fig. 4 and Table 5).

## **5. Diurnal, weekly and annual variations of pollutants with land-use types**

Figure 5 shows the spatial distributions of climatological annual averages in a 0.25°×0.25° grid over South Korea during 2002-2013 of the surface air pollutant observations for O<sub>3</sub> (ppb), CO (0.1 ppm), NO<sub>2</sub> (ppb), SO<sub>2</sub> (ppb) and PM<sub>10</sub> (μg m<sup>-3</sup>) in terms of the MEK four land-use types of a) residence, b) commerce, c) industry and d) greenbelt. The distributions present unique characteristics by the four land-use types. For instance, Seoul, where both the residence and commerce types were dominant, was the most polluted with the CNSP pollutants in all of the land-use types. The CO was higher inland than in the coastal

areas and the  $\text{NO}_2$  was higher in the major cities including Seoul, Daegu, and Busan for all of the types. The distribution of  $\text{SO}_2$  was similar to that of  $\text{NO}_2$ , but the former was larger in the coastal area than the latter due to its industry emissions. On the other hand,  $\text{O}_3$  levels in the greenbelt type were the highest among the four types (Fig. 5d).

Figure 6 presents the (a) diurnal, (b) weekly and (c) annual variations in the spatial averages of Fig. 5 under the MEK four land-use types as follows; residence (black circle), commerce (blue cross), industry (red square), and greenbelt (green triangle). The diurnal variations of four kinds of pollutants were investigated in the previous studies by Flemming et al. (2005) and Meng et al. (2009). The former study also showed their weekly and annual variations over different air-quality regimes, while the latter emphasized significant seasonality in their diurnal cycles. In addition, Xu et al. (2008) investigated interannual variability of the surface  $\text{O}_3$  in its diurnal cycle in four different seasons. In this study, the diurnal cycles of the five pollutants were analyzed for the different land-use regime. The results in the figure are also summarized in Tables 6-7. Table 6 shows the magnitude order of the five pollutant concentration averages of Fig. 6 in terms of the land-use types. The numbers in the table indicate the ranking of each pollutant based on the pollutant concentration values over the types. The greater concentration values corresponded to the upper ranking numbers. Only if the orders in the two types of grids were different from each other, then those in the parentheses were given for the  $0.1^\circ \times 0.1^\circ$  grid. Table 7 also presents the spatial mean and standard deviation of the averages in a  $0.25^\circ \times 0.25^\circ$  grid. The values in parentheses in the table denote the mean and standard deviation in a  $0.1^\circ \times 0.1^\circ$  grid.

The typical shapes of the diurnal, weekly and annual cycles of the five pollutants were quite similar among the different land-use types but their magnitudes were systematically different depending on the types (Fig. 6 and Tables 6-7). In other words, the rank of the pollution level by the land-use type in the weekly and annual cycles was almost the same as in the diurnal cycle (Tables 6-7). In Table 6, the magnitude order ( $G > R > I > C$ ) for  $\text{O}_3$  with the types was exactly in the reverse order for  $\text{NO}_2$  ( $C > I > R > G$ ) for all cycles, suggesting the linkage between the two pollutants. The anti-correlations between the two pollutants in the diurnal cycle were also shown in Mazzeo et al. (2005) at a green city of Argentina and Han et al. (2011) in Tianjin, China. However, the reverse order for  $\text{O}_3$  was different from those for  $\text{SO}_2$  and  $\text{PM}_{10}$  ( $I > C > R > G$ ). It is because  $\text{SO}_2$  and  $\text{PM}_{10}$  pollutants were not uniquely associated with vehicle emissions (Flemming et al., 2005; see also Chen et al., 2001). The

same order for the two pollutants with the land-use types suggested their emission sources from industrial activities rather than traffic emissions. It was interesting to note that the greenbelt area was commonly the lowest for the CNSP pollutants.

Since the primary production of O<sub>3</sub> was through photochemical reactions, the O<sub>3</sub> started to rise in the morning and showed its peak at 4 p.m. before it rapidly decreased (Fig. 6a). The O<sub>3</sub> level was the highest in the greenbelt and the lowest in the commerce areas, while the levels of the O<sub>3</sub> for the residence and industry regimes were close to each other. The diurnal cycle of the O<sub>3</sub> in this study agreed with that of Flemming et al. (2005). Two peaks were shown in the diurnal cycle for CO, NO<sub>2</sub>, and PM<sub>10</sub>. The first peak was due to the increasing morning traffic and industrial activity (Kuttler and Strassburger, 1999). The second peak was due to the afternoon traffic and reduced boundary layer (Lee et al., 2014) during and after sunset. The daytime minima of these species were the results of the increased boundary layer height (Ulke and Mazzo, 1998; Lal et al., 2000; Han et al., 2011) as well as the oxidation processes for the chemically and photochemically reactive CO and NO<sub>2</sub> of which diurnal variations were generally out of phase with those of O<sub>3</sub> except for the midnight period (Kuttler and Strassburger, 1999; Lal et al., 2000). The diurnal cycle of the SO<sub>2</sub> in the commerce type also had two peaks similar to the other pollutants (CO, NO<sub>2</sub> and PM<sub>10</sub>). The daytime minima could be explained by the high vertical mixing of their emissions (Meng et al., 2009). According to the diurnal variations of the CO and SO<sub>2</sub> over a suburban site in the USA, the patterns of their diurnal cycles were changed seasonally (Chen et al., 2001). The diurnal cycles of the O<sub>3</sub> and NO<sub>2</sub> without categorizing the land-use types were shown in Fig. 6a (O<sub>3</sub> and NO<sub>2</sub>), consistent with those of Han et al. (2011) in Tianjin, China.

The commerce type in the daily, weekly, and annual cycles was ranked first for the CO and NO<sub>2</sub>, but it was ranked second for the SO<sub>2</sub> and PM<sub>10</sub> (Fig. 6 and Table 6). The industry type was ranked first for the SO<sub>2</sub> and PM<sub>10</sub>, but it was ranked second for the NO<sub>2</sub>. The residence type in a 0.25°×0.25° grid was ranked second with the industry regime for the CO, but it was ranked third for the NO<sub>2</sub>, SO<sub>2</sub>, and PM<sub>10</sub>. These analyses indicated that the contribution of commerce was more important for the CO and NO<sub>2</sub>, and that the contribution of the industry was more important for the SO<sub>2</sub> and PM<sub>10</sub>. Since the commerce and industry types were associated with more vehicles and industrial activity, the CNSP pollutants in the residence type were lower than for these two types. Sharma et al. (2014) also reported that the

PM<sub>10</sub> levels in South Korea and abroad depended on different land-use types (urban, industry, rural/suburban).

The weekly cycles were analyzed for the different land-use types (Fig. 6b). The weekly cycle of the five pollutants was more remarkable in the land-use types with industrial and commercial activities, particularly in the industry type than in the greenbelt one. The CO weekly cycle was pronounced in the commerce type as well as in the industry one. This implies that the MEK land-use types provided a reasonable discrimination between natural and anthropogenic pollutant sources. In general, on Sunday the level of the CNSP pollutants decreased but the O<sub>3</sub> values showed a peak. However, the degree of the Sunday pollutant values compared to those averaged for the working days from Tuesday to Friday (hereafter the working day average) varied by the pollutant species and land-use types. These Sunday low of the CNSP pollutants and the Sunday high of O<sub>3</sub> (so-called the O<sub>3</sub> weekend effect; Larsen et al., 2003) were due to the anthropogenic activity that characterized the weekly emission pattern of South Korea.

In Fig. 6b for O<sub>3</sub>, less O<sub>3</sub> reduction near anthropogenic sources (e.g., the commerce and residence areas) due to the decreased NO titration could induce an enhancement of O<sub>3</sub> particularly in the weekly cycle (e.g., Gilge et al., 2010). The NO<sub>2</sub> minimum on Sunday also occurred in Hohenpeissenberg, Germany due to less anthropogenic impact on weekends than on working days (Gilge et al., 2010). In Fig. 6b, the NO<sub>2</sub> minimum on Sunday (24% reduction compared to the working day average) in the industry agreed with that of Beirle et al. (2003) over the industrialized regions (the USA, Europe and Japan) from the vertical column densities of tropospheric NO<sub>2</sub>. The CO reduction on Sunday against the weekday average was the lowest (3-7%) among the CNSP due to its longer life time (e.g., Gilge et al., 2010). The PM<sub>10</sub> minimum on Sunday also occurred over a neighboring country, China (Choi et al., 2008). The O<sub>3</sub> Sunday maximum in the industry type was enhanced by ~15% with respect to the weekday average. The weekend effect of O<sub>3</sub> varied with the land-use types: I (15%) > C (10%) > R (9%) > G (4%). The increasing O<sub>3</sub> during the weekend could be associated with: 1) the decreasing NO<sub>2</sub> under the VOCs-limited regime, or 2) the behavior of the VOCs (e.g., Sakamoto et al., 2005), particularly the natural ones (or biogenic) in the greenbelt. Previous studies showed an increase in the O<sub>3</sub> and a decrease in the NO<sub>2</sub> during the weekends in the U.S. and Germany (Flemming et al., 2005; Atkinson-Palombo et al., 2006).

According to Gilge et al. (2010), anti-correlation between O<sub>3</sub> and NO<sub>2</sub> in their weekly cycles was less pronounced in summer due to photochemical O<sub>3</sub> production than in the other seasons.

The annual cycle of O<sub>3</sub> generally showed a spring-early summer maximum and a wintertime minimum (Fig. 6c). This result was consistent with that of Pochanart et al. (1999) at Oki, Japan and on a regional scale in northeast Asia. The O<sub>3</sub> annual variation in the greenbelt presented primary and secondary peaks in May and October, respectively, reflecting seasonal changes of the photochemical intensity and Asian monsoon (Meng et al., 2009; Sarangi et al., 2014). The double peak patterns occurred at a regional background site in northern China in June and September, respectively (Meng et al., 2009), and at a high altitude site in north India in May and November, respectively (Sarangi et al., 2014). However, the secondary peak was not clear in the other types (residence, commerce and industry). This suggested that the O<sub>3</sub> production in a monthly time-scale was sensitive to the local pollutant emissions with the land-use types. The NO<sub>2</sub> wintertime maxima could be associated with the fossil fuel consumption and photochemical oxidation of NO to NO<sub>2</sub> (Shon and Kim, 2011), the lower planetary boundary layer (PBL) and photolysis rate. The enhanced CO and NO<sub>2</sub> values in winter agreed with those of Gilge et al. (2010) over Hohenpeissenberg, Germany. Tropospheric NO<sub>2</sub> concentrations over South Korea also occurred in winter (at least 68%) mainly due to local emissions (Mijling et al., 2013).

The SO<sub>2</sub> maximum in January in its annual cycle was generally similar to that of SO<sub>2</sub> emissions from China of Wang et al. (2013) (Fig. 6c). The values of the CNSP pollutants were lowest in June-August mainly due to the washout effect during the rainy period (e.g., Flemming et al., 2005; Meng et al., 2009; Yoo et al., 2014). Despite the low washout effect of CO, its reaction with HO radical was likely to be more important for the CO sink during the warm season (Stockwell and Calvert, 1983; Novelli et al., 2003; Gilge et al., 2010). The declining tendency of the SO<sub>2</sub> and NO<sub>2</sub> emissions in boreal summer also occurred in China because of the large-scale monsoon system (Wang et al., 2013). In addition, the lifetimes of SO<sub>2</sub> and NO<sub>2</sub> in the atmosphere are substantially shorter in summer, due to dominant gas phase chemistry (e.g., faster photochemical reactions) (Levy II et al., 1999). This implies that the NO<sub>2</sub> transport from China to South Korea could have more impact over the Korean Peninsula during wintertime dry season than during the summer and fall (Lee et al., 2014). The springtime PM<sub>10</sub> maxima in its annual variations resulted from Asian Dust and meteorological conditions (Sharma et al., 2014).

In the annual average analyses, the urban effects of the grid difference (i.e., the pollutant value in the  $0.1^\circ \times 0.1^\circ$  grid minus the value in the  $0.25^\circ \times 0.25^\circ$  grid) was quantitatively the greatest in the types of ‘commerce’ for CO (+0.093 0.1ppm), NO<sub>2</sub> (+2.969 ppb), PM<sub>10</sub> (+0.711  $\mu\text{g m}^{-3}$ ), and O<sub>3</sub> (-0.735 ppb); and ‘industry’ for SO<sub>2</sub> (+0.687 ppb) among the four land-use types (Table 8). This result could be explained by the emissions of vehicle in the commerce type and the emissions of factories in the industry type.

## 6. Pollutant trends of O<sub>3</sub>, NO<sub>2</sub>, SO<sub>2</sub>, CO, PM<sub>10</sub>, and OX with respect to land-use types

Figure 7 shows the time series of the spatial averages of the monthly surface air pollutant anomalies for the five pollutant and OX concentrations in a  $0.25^\circ \times 0.25^\circ$  grid over South Korea during the period from January 2002 to December 2013 under the following MEK land-use types: residence (black solid), commerce (blue dashed), industry (red dotted), and greenbelt (green dashed). We calculated linear trends of the pollutant anomalies with respect to each of the land-use types. The  $\pm$  trend values define the 95% confidence intervals. Trend values of the pollutants are also summarized in Table 9, based on two types of analyses (the  $0.1^\circ \times 0.1^\circ$  and  $0.25^\circ \times 0.25^\circ$  grids) over the four land-use types of MEK of residence (R), commerce (C), industry (I), and greenbelt (G). The magnitude order for the trends of each of the pollutant over the types has been shown. It should be noted that the trend values were statistically significant except for a few of the NO<sub>2</sub> and SO<sub>2</sub> cases marked by an asterisk (\*). Given the different spatiotemporal scales of the variability for the five pollutants (their scale order; CO > PM<sub>10</sub> > O<sub>3</sub> > SO<sub>2</sub> > NO<sub>x</sub>; Seinfeld and Pandis, 2006), the behavior of CO was likely to be related with the local, regional, and global effects but that of NO<sub>2</sub> with the local and regional ones (Gilge et al., 2010).

The CNSP pollutants in South Korea tended to decrease regardless of the land-use types but interestingly the O<sub>3</sub> had an increasing tendency (Fig. 7 and Table 9). Since the five pollutants showed the same trends (either positive or negative) over all of the four types, the overall trends could reflect more the effects of regional emissions than local emissions. In the O<sub>3</sub> formation, for instance, the local contribution related with the level of primary pollutants (e.g., titration) while the regional contribution corresponded to the background O<sub>3</sub> concentration (Clapp and Jenkin, 2001). The regional background was likely to be large in the greenbelt area compared to the other land-use types in view of the reduced weekly cycle



in the greenbelt (see also Fig. 6b). The declining trends of CNSP in a  $0.25^\circ \times 0.25^\circ$  grid by the land-use type varied with the values of  $-0.135 \sim -0.247$  ( $0.1 \text{ ppm yr}^{-1}$ ) for CO,  $-0.042 \sim -0.295$  ( $\text{ppb yr}^{-1}$ ) for NO<sub>2</sub>,  $-0.036 \sim -0.140$  ( $\text{ppb yr}^{-1}$ ) for SO<sub>2</sub>, and  $-1.003 \sim -1.098$  ( $\mu\text{gm}^{-3} \text{ yr}^{-1}$ ) for PM<sub>10</sub>.

The downward trend of PM<sub>10</sub> ( $\sim 2 \text{ \%yr}^{-1}$ ) in this study agreed with the result ( $0.4 \sim 2.7 \text{ \%yr}^{-1}$ ) in Sharma et al (2014) over major cities in the country during 1996-2010 (Fig. 7f and Table 9). The largest decrease for CO and SO<sub>2</sub> in the industry type was due to the reduced emissions from factories and power plants (Fig. 7d and e); the largest decrease for NO<sub>2</sub> in the residence type was associated with the reduced emission from vehicles (Fig. 7b); the commerce type was second (CO and SO<sub>2</sub>) and third (PM<sub>10</sub>); and the CNSP trends in the greenbelt type were low (third or fourth) except for PM<sub>10</sub>. However, there was almost no difference in the PM<sub>10</sub> declining trend between the land-use types. Kim and Shon (2011) reported that the sudden increase of PM<sub>10</sub> in spring 2002 occurred due to the enhanced Asian Dust effect. The systematic decreasing trend of the CNSP pollutants suggested that the policy for air quality regulation worked successfully (Sharma et al., 2014).

In contrast to the CNSP case, it was interesting that the O<sub>3</sub> value in a  $0.25^\circ \times 0.25^\circ$  grid increased with the rate of  $0.352 \sim 0.501$  ( $\text{ppb yr}^{-1}$ ;  $\sim 1.6\%$ ) over the last 12 years although the CNSP pollutants were reduced (Fig. 7 and Table 9). This phenomenon was consistent with Mayer (1999), who reported that long-term trends of major air pollutants except for O<sub>3</sub> were decreasing, particularly in industrialized countries, but global O<sub>3</sub> levels were increasing during the early period of the twenty-first century (Cooper et al., 2010). On the other hand, the standards of the surface O<sub>3</sub> concentration for its government control in South Korea are less than 0.1 ppm for the O<sub>3</sub> average during one hour, and less than 0.06 ppm for the O<sub>3</sub> average during eight hours (NIER, 2010). Furthermore, one of three stages of ozone warning in the region is issued, based on the surface O<sub>3</sub> concentration; ozone alert for  $0.12 \text{ ppm hr}^{-1}$  or higher, ozone warning for  $0.3 \text{ ppm hr}^{-1}$  or higher, and ozone grave warning for  $0.5 \text{ ppm hr}^{-1}$  or higher concentration. While surface O<sub>3</sub> level varies seasonally from 0.018 ppm in winter to 0.035 ppm in spring in South Korea (Table 5), there have been 84 times for 28 areas of the ozone alert, and 83 times for 27 areas of the ozone warning on an annual basis during the 12-year period of this study (<https://seoulsolution.kr/content/ozone-warning-system-ozone-warning-system-protect-citizens%E2%80%99-health?language=en>). Given the increasing trends of O<sub>3</sub> found in this study (Fig. 7a), it will be important to understand possible factors causing such trends. Seo et al. (2014) reported an increase in the O<sub>3</sub> ( $+0.26 \text{ ppb yr}^{-1}$ ) in 46

cities in South Korea from 1999 to 2010. Also the O<sub>3</sub> increase (+0.48 ppb yr<sup>-1</sup>) from 1990 to 2010, which was more consistent with our results, generally occurred for all of the seasons and day/night at most of the surface monitoring sites (Lee et al., 2014). This tendency was commonly shown in the two types of spatial grid analyses, possibly due to growing background O<sub>3</sub> (Table 9).

The possibility of enhanced regional (background) O<sub>3</sub> as well as the local effect of the O<sub>3</sub> titration could be supported by the significant upward trends (0.205-0.396 ppb yr<sup>-1</sup>; Table 9 and Fig. 7c) of the total oxidant (OX) despite the downward trends of the O<sub>3</sub> precursors (e.g., NO<sub>2</sub>, CO, and PM<sub>10</sub>). Specifically the significant positive trends of the OX values (0.260-0.300 ppb yr<sup>-1</sup>) in the greenbelt type in the two kinds of spatial grids suggested the increase of background O<sub>3</sub> induced by its inflow from the regional scale, rather than the local scale. The upward trends of the OX in the both grids were commonly more pronounced in the commerce type than the other types, but the cause was unknown.

A positive trend of tropospheric ozone (3.1% yr<sup>-1</sup>) was clearly seen over Beijing from 2002-2010 in Wang et al. (2012), who emphasized a contribution in the downward O<sub>3</sub> flux from the stratosphere for the period. In spite of the CNSP decreasing trends in a 0.25°×0.25° grid (i.e., less urban features), the NO<sub>2</sub> tendency in a 0.1°×0.1° grid (i.e., more urban features) was not evident except for the residence (Table 9). Thus, the government regulation for NO<sub>2</sub> might not be very successful in large cities due to its diverse sources. Xu et al. (2008) suggested that the increased variability of the surface O<sub>3</sub> at a station in eastern China were mainly associated with the enhanced NO<sub>x</sub> emission near the station.

The O<sub>3</sub> levels, which were related to the spatial variability in the local precursor emissions, were expected to vary with the land-use types. Seo et al. (2014) revealed that the long-term trends of the local precursor emissions on O<sub>3</sub> in South Korea could affect the O<sub>3</sub> trends locally, and in the country, significant enhancement of the background O<sub>3</sub> negatively affected the air quality. In order to understand the negative relationship in trend between O<sub>3</sub> and CNSP pollutants, particularly NO<sub>2</sub>, we have investigated the relationship (i.e., correlation and weekly cycle) among O<sub>3</sub>, NO<sub>2</sub> and VOCs with the land-use types further in sections 6 and 7. In this study, we focused on two issues: 1) which condition in view of the O<sub>3</sub> control in South Korea was more dominant, the VOCs-sensitivity or NO<sub>2</sub>-sensitivity? 2) Did this condition significantly depend on the land-use types and the weekly cycles of the pollutants? The negative relationship between O<sub>3</sub> and NO<sub>2</sub> is expected in the VOCs-limited condition.

Local effect of the pollutants compared to the regional (i.e., background) effect can be shown, based on their weekly variations at each station of the four land-use types.

## 7. Correlation between O<sub>3</sub> and NO<sub>2</sub> with land-use types

As shown in Fig. 7, the increasing O<sub>3</sub> trend was the opposite of the decreasing CNSP trends. The O<sub>3</sub> trends could be affected by interannual variations of the pollutant emissions (e.g., NO<sub>x</sub> and VOCs) from their various sources and of the meteorological conditions (Kim et al., 2006). In view of the ‘O<sub>3</sub> control’ strategy, the relationship between O<sub>3</sub> and NO<sub>x</sub> (and the VOCs) was examined in many previous studies (e.g., Mazzeo et al., 2005; Han et al., 2011). There were various factors affecting the O<sub>3</sub>: 1) local precursor emissions (e.g., NO<sub>2</sub>, VOCs, and CO, etc.); 2) O<sub>3</sub> transport and its precursors from the local and remote sources; and 3) meteorological conditions (Seo et al., 2014). In this study we focused on the relationships on the local (grid) and regional (nationwide) scales in South Korea.

Figure 8 shows scatter diagrams of the O<sub>3</sub> versus NO<sub>2</sub> from the monthly anomalies of Fig. 7 in South Korea under the four land-use types: a) residence (black circle), b) commerce (blue cross), c) industry (red square) and d) greenbelt (green triangle). The sample number in the monthly anomaly time series of each pollutant was 144 during 2002-2013. The temporal correlation coefficient ( $r$ ) between the anomalies of the two pollutants was given together with the regression dotted line. The correlations in the residence and commerce types were statistically significant at a significance level of  $p < 0.01$  (i.e., either  $r > 0.194$  or  $r < -0.194$ ). The correlation was also significant at  $p < 0.05$  (i.e., either  $r > 0.137$  or  $r < -0.137$ ) in the industry type, but not significant in the greenbelt type due to the least NO<sub>2</sub> emissions. Therefore, these results indicated that the NO<sub>2</sub> emissions from vehicles in the residence and commerce areas were highly related to the O<sub>3</sub> change on the long-term time scale (Fig. 8a-b). Also the NO<sub>2</sub> probably affected the O<sub>3</sub> in the industry type. The above results agreed with those of Seo et al. (2014) who reported that the long-term O<sub>3</sub> variation over South Korea was similar to that of NO<sub>2</sub>, but their trends were spatially different.

Figure 9 presents the relationship between O<sub>3</sub> and NO<sub>2</sub> in terms of the climatological annual averages over South Korea during 2002-2013 under the MEK four land-use types of: residence (R), commerce (C), industry (I), and greenbelt (G). The relationship was derived from the data all of the 283 stations, which were individually specified by one land-use type

among the four types (Fig. 9a). Since the stations of residence were located nationwide (i.e., more than a half of all the stations), the relationship could be spatially different due to the population-related traffic emissions. Furthermore, the NO<sub>2</sub> decreasing trends in a 0.1°×0.1° grid (Table 9) were found significant only in the residence area, but not in the other types, despite the government control efforts (e.g., Shon and Kim, 2011). Note that the pollutant trends in a 0.25°×0.25° grid were given in Fig. 7, where the NO<sub>2</sub> trends were significant except for the commerce among the four land-use types. In order to further investigate the relationship within the residence areas based on the population size, we subdivided the locations of the 154 residence-type stations of Fig. 1a by the three regions (Fig. 9b) as follows: i) the capital city of the country, Seoul (red circle), ii) the SMA (green circle) except for Seoul, and iii) outside of the SMA (blue circle). Therefore, the SMA is composed of i) Seoul and ii) the SMA except for Seoul. The 20% and 50% portions of the entire population in South Korea (~50.5 million in 2014) lived in Seoul and the SMA, respectively. There were more traffic emissions in the SMA than outside of the SMA, particularly in the residence types.

A very strong correlation ( $p < 0.01$ ) of PM<sub>10</sub> with the CO and NO<sub>2</sub> in their monthly dataset time series (Fig. 7) was likely to be associated with the traffic emission sources (see also Shon and Kim, 2011; Sharma et al., 2014). The correlations (0.42-0.56) in the residence and commerce were greater than those (0.32-0.47) in the greenbelt and industry, which was probably due to the vehicle emissions. In other words, more traffic emissions, which were related to the population density, were expected in Seoul than in the SMA excluding the capital city. The residence and commerce types were dominant in Seoul (Fig. 1a-b), while the residence and industry types predominantly existed in the SMA (Fig. 1b and d). Figure 9c is the same as Fig. 9a except for excluding the data in the SMA residence areas. Figure 9d is the same as Fig. 9a except for the O<sub>3</sub> and NO<sub>2</sub> relationships in the residence only over the three different regions shown in Fig. 9b. In Fig. 9d, the relationships over the three regions are shown in three colors, respectively.

The NO<sub>2</sub> value was the highest in the commerce areas over South Korea (Fig. 9a and c; Table 10). The NO<sub>2</sub> concentration was estimated in the following order: Commerce (C; 31.3) > Residence (R; 25.9) > Industry (I; 24.3) > Greenbelt (G; 13.3) (Fig. 9a). However, when the NO<sub>2</sub> (ppb) values in the region excluding the 74 SMA residence stations were examined, the order of the residence and industry areas was different from the previous case as follows:

I (24.3) > R (20.3) (Fig. 9c). This result suggested that there were more NO<sub>2</sub>-related traffic emissions (5.6 ppb) in the SMA residence areas than in the nationwide residence areas (Fig. 9a and c). The maxima (30.2 ppb) of the O<sub>3</sub> concentrations occurred in the greenbelt areas, while their minima were shown in the commerce areas (Fig. 9a and c). The order of magnitude of the O<sub>3</sub> was the opposite of that of the NO<sub>2</sub>, showing an inverse relationship between the two pollutants (see also Han et al., 2011).

The traffic-induced pollutants were mainly NO, CO and PM<sub>10</sub>, as well as VOCs, and the secondary trace gases of O<sub>3</sub> and NO<sub>2</sub> could be formed from these precursor substances during the photochemical reactions (Kuttler and Strassburger, 1999). They reported the inverse relationship of the O<sub>3</sub> versus NO<sub>2</sub> within the urban areas (Essen, Germany) with the following five land-use types: motorway, the main and secondary roads, residence and greenbelt. The three types of the roads and motorway could correspond to the commerce areas in our study, particularly in the urban area (e.g., the SMA). Overall, our results were consistent with those of Kuttler and Strassburger (1999) who showed that the higher O<sub>3</sub> concentration was formed in urban green areas in the summer during intensive solar radiation, due to the relatively low share of NO in the total concentrations of NO<sub>2</sub> in the greenbelt areas. However, an inverse relationship has been also found in winter (Table 10). The consistency in the relationship of O<sub>3</sub> versus NO<sub>2</sub> between the two studies supported the validation of the MEK classification method for the four land-use types. According to the monthly mean analysis of Xu et al. (2008) at a background station in eastern China, the negative correlation between O<sub>3</sub> and NO<sub>x</sub> was found in the lowest 5% of ozone in cold season than in the highest 5% in warm season. Overall, the inverse relationship in Fig. 9a and c of this study, which systematically showed in the O<sub>3</sub> magnitude order (G > R > I > C; see also Table 6 in a 0.25°×0.25° grid) over the stations excluding the SMA residence areas in a non-grid, agreed well with the previous studies, suggesting that the four MEK land-use type classification was made reasonably.

As shown in Figs. 1a and 9a, the number of nationwide residence stations was the largest among the four land-use types. The spatial dependence of the O<sub>3</sub> versus NO<sub>2</sub> relationship over the three different residence types (Fig. 9b; Seoul, the SMA except for Seoul, and Outside of the SMA) where the amounts of traffic emissions were expected to be different due to the number density of automobiles per unit area (as shown in Fig. 1d) was interesting to note. Furthermore, relatively short-lived NO<sub>2</sub> compared to the other pollutants

(CO, PM<sub>10</sub>, O<sub>3</sub>, and SO<sub>2</sub>) in this study was used as a good indicator to reflect local and regional anthropogenic effects (Gilge et al., 2010). Although the SMA included Seoul, the residence region was separated into two sub-regions in this study in order to analyze the difference in the pollutants between them (Fig. 9d and Table 10). Heavier traffic generally occurred in Seoul than in the rest areas in the SMA. The NO<sub>2</sub> (ppb) concentrations in the residence areas over South Korea were estimated in the following order: Seoul (35.5±2.53) > SMA except for Seoul (31.7±4.03) > Outside of the SMA (20.3±4.94) (Fig. 9d). In the residence, there were pronounced reductions in the mean and standard deviation values of NO<sub>2</sub> due to the greater distance from the main traffic-induced pollution sources in the SMA including Seoul. The order of the O<sub>3</sub> (ppb) concentrations was the opposite of that for the NO<sub>2</sub> as follows; Outside of the SMA (25.0±4.03) > SMA except for Seoul (19.8±1.74) > Seoul (18.6±1.30). As a result, the MEK residence type, which had large variations in the two pollutant concentrations, could be required to be subdivided in the future in view of the O<sub>3</sub> versus NO<sub>2</sub> relationship. However, the difference in the concentrations between the two regions within the SMA (i.e., Seoul and the SMA except for Seoul) was relatively small compared to that between the SMA and outside of the SMA, due to their transport over the geographically neighboring locations.

## **8. Weekend effect of the O<sub>3</sub>, NO<sub>2</sub>, VOCs, OX, and VOC/NO<sub>2</sub> with land-use types**

Since the O<sub>3</sub> formation at the surface can depend on two major precursors (i.e., NO<sub>x</sub> and VOCs; Larsen et al., 2003) and the ratio of the NO<sub>x</sub> and VOCs (e.g., Pudasainee et al., 2006), the relationship among these three pollutants (O<sub>3</sub>, NO<sub>2</sub> and VOCs) was examined in the weekly cycles of many previous studies (e.g., Gilge et al., 2010). The impact of the VOCs emission controls on the O<sub>3</sub> trend in northwest Europe was discussed in Derwent et al. (2003). Both the VOC emission data and the observations of atmospheric concentrations of VOCs in South Korea were lacking compared to those of the O<sub>3</sub> and NO<sub>2</sub>, and thus the VOC observational sites and records were sparse (as shown in Fig. 1e and Table 2). Figure 10 shows the weekly variations in the VOCs (green triangle), O<sub>3</sub> (red square) and NO<sub>2</sub> (blue rectangle) concentrations at 9 photochemical air pollution monitoring stations in South Korea since 2007 under the MEK four land-use types. The land-use types at the stations available for simultaneous observations (O<sub>3</sub>, NO<sub>2</sub>, and VOCs) were 4 residences (the sites of Bulgwang,

Daemyoung, Gocheon and Goowol), 3 greenbelts (Seokmo, Taejong and Gwanin), a commerce area (Simgok) and an industry area (Joongheung).

The weekly cycle of the three pollutants was conspicuous in the residence and commerce areas (Fig. 10a-e). In the areas, the  $\text{NO}_2$  and VOCs values were higher by 20-33% on the weekdays than on the weekends due to variations in anthropogenic activity, while the  $\text{O}_3$  value was higher by 17-21% on the weekends. The VOCs increase on weekdays in the residence (Bulgwang) was probably due to vehicle emissions (e.g., Anthwal et al., 2010). The so-called weekend effect has been reported by Marr and Harley (2002a, 2002b) and Fujita et al. (2003a, 2003b) over the LA basin with higher  $\text{O}_3$  concentrations on the weekends than on the weekdays. Marr and Harley (2002b) also found the weekly patterns of the lower  $\text{NO}_x$  and VOCs during weekend, out of phase with the higher  $\text{O}_3$ . Qin et al. (2004b) revealed that VOCs-limited condition for  $\text{O}_3$  production and the  $\text{NO}_x$ -emission reduction in weekend could be associated with the weekend effect of  $\text{O}_3$  in Southern California. In contrast to the residence and commerce areas, however, the weekly cycles of the three pollutants are not clear in the greenbelts and industry areas (Fig. 10f-i). In view of the negligible weekly cycle in the industry areas (Fig. 10f), the primary source for the cycle was traffic emission rather than the industrial factory activity. Since the industry station at Joongheung was located near the coast (Fig. 1e; red square), it could also have been influenced by meteorological factors (e.g., sea breeze). In addition, more observations for the industry and commerce types were required for detailed analysis, because the photochemical (VOCs) data in the two types were only available at a single station, respectively (Fig. 10 e-f). In summary, more local effect influenced on the three pollutants in the residence and commerce areas, while regional (background) effect dominated in the greenbelt and industry areas.

It is interesting to note that the averages of the three pollutants at Simgok in the commerce (Fig. 10e) were highly contrast with those at Seokmo (Fig. 10g) in the greenbelt type. In other words, the  $\text{O}_3$  level among the nine stations (Fig. 10) was the highest at Seokmo but relatively low at Simgok. However, the  $\text{NO}_2$  and VOCs values had an opposite tendency with the  $\text{O}_3$  case, showing their high values at the former (commerce) site and their low values at the latter (greenbelt) site. According to the study of Seo et al. (2014), larger  $\text{NO}_x$  emissions over the metropolitan cities in the short-term and seasonality showed lower  $\text{O}_3$  minima because of  $\text{NO}_x$  titration and a nocturnal  $\text{NO}_y$  chemical process. They also

reported that the higher O<sub>3</sub> level near the Seokmo greenbelt (i.e., Ganghwa) were induced due to lower NO<sub>x</sub> emissions and the regional O<sub>3</sub> influxes from both the Yellow Sea (and China) and the SMA.

The decrease of local VOCs reduced O<sub>3</sub> with a reasonable amount of NO<sub>2</sub>, and the ratio of VOCs to NO<sub>x</sub> (i.e., VOC/NO<sub>x</sub>) was an important factor for the O<sub>3</sub>-control strategy (Marr and Harley, 2002a, 2002b; Fujita et al., 2003a, 2003b). Decreasing NO<sub>x</sub> tended to increase O<sub>3</sub> formation when the VOC/NO<sub>x</sub> ratio was less than the threshold values of 8-10 (Larsen et al., 2003). In addition, decreasing NO<sub>x</sub> tended to decrease O<sub>3</sub> formation when the ratio was greater than the threshold values. In this study, the NO<sub>2</sub> value instead of NO<sub>x</sub> was introduced for an approximate calculation of the ratio. The amounts of NO<sub>2</sub> approximately corresponded to 77-95% of the amount of NO<sub>x</sub> over a background station in northern China (Meng et al., 2009). Therefore, the ratios used in this study (i.e., VOC/NO<sub>2</sub>) may be overestimated, compared to those of VOC/NO<sub>x</sub>. The inter-relationship among the three pollutants was statistically examined in view of the individual role of NO<sub>2</sub> and VOCs for the O<sub>3</sub> control in this study. Figure 11 shows the scatter diagrams of the long-term averages of the a) VOCs vs. NO<sub>2</sub>, b) O<sub>3</sub> vs. VOCs, c) O<sub>3</sub> vs. NO<sub>2</sub>, and d) O<sub>3</sub> vs. VOC/NO<sub>2</sub> at the photochemical stations under the following four land-use types; residence (black circle), commerce (blue cross), industry (red square), and greenbelt (green triangle). The correlation coefficient and the dotted regression line were also given. The spatial coefficients were statistically significant for the cases of O<sub>3</sub> vs. NO<sub>2</sub> at  $p < 0.01$  (i.e.,  $r < -0.750$ ; Fig. 11c) and for VOCs vs. NO<sub>2</sub> at  $p < 0.05$  (i.e.,  $r > 0.583$ ; Fig. 11a). Meanwhile the correlations were not significant for the other two cases (O<sub>3</sub> vs. VOCs, and O<sub>3</sub> vs. VOC/NO<sub>2</sub>) (Fig. 11b and d). The significant positive correlation between the VOCs and NO<sub>2</sub> might have been due to their common anthropogenic sources (e.g., transportation and industrial activities, etc). Nine VOC values in Fig. 11a-b were systematically separated by their types in view of magnitude. However, the residence values for the NO<sub>2</sub> and O<sub>3</sub> cases were not distinct from the industry case, due to their broad-range values in the residence areas (Fig. 11c). Overall, the pollutant values at the 4 residences and 3 greenbelts are systematically clustered in the 2-dimensional domains of Fig. 11, supporting the idea that the MEK land-use types are reasonable.

Figure 12 presents weekly variations of the OX and VOC/NO<sub>2</sub> values at each of the 9 photochemical stations of Fig. 10. The equally-weighted averages with respect to the four land-use types were also given for the OX and VOC/NO<sub>2</sub> in Fig. 12a-b (the grey cross dashed



line), respectively. The weekend effect of OX in the residence and commerce was evident, while it was negligible in the greenbelt area (Fig. 12a). This contrast suggested the reduction of order of OX (ppb) is C (57.4) > R (53.6) > I (50.7) > G (45.4) (Table 11). The weak weekly cycle of OX in the greenbelt may be associated with the OX background level, although there was about a 9 ppb difference in OX between the greenbelt stations.

The average of VOC/NO<sub>2</sub> (the grey cross dashed line) did not show a clear weekly cycle (Fig. 12b). The weekly cycles of the ratio were almost negligible except for some stations. The industry type at Joongheung had a minimum on Tuesday in the weekly cycle, and its cause was unknown. Some weekend effects of the reduced ratio (i.e., the decrease on Saturday-Monday) at Daemyoung and Gocheon in the residence area occurred possibly due to the NO<sub>2</sub> reduction from less anthropogenic traffic emission. The ratio values tend to be relatively low in the greenbelt (2.0-5.3) and residence (2.6-3.5) areas. The four type average was 6.6 (Table 11). Based on the average result at the photochemical stations, the VOCs-limited chemistry over South Korea was more common than the NO<sub>x</sub>-limited one in the industry (Joongheung). As a result, except for the Joongheung station, the NO<sub>2</sub> decrease in weekend could result in the enhanced O<sub>3</sub> production at the other eight stations in South Korea. This phenomenon was more conspicuous in the residence and commerce areas (5 stations) due to the weekly cycle of anthropogenic vehicle emission than in the greenbelt areas (3 stations). The ratio result in this study over the SMA was consistent with that of Jin et al. (2012) who reported that the areas of the Seoul and Incheon cities were VOCs-limited using the Ozone Isopleth Plotting Package for Research (OZIPR) model. Also in the model study, 24 areas in Gyeonggi-do where approximately included the SMA except the two cities was equally either VOCs-limited or neutral. However the modelling had some limitations due to inaccuracy in emission inventories and transport.

Figure 13 and Table 11 summarized the long-term surface air pollutant averages (O<sub>3</sub>, NO<sub>2</sub>, OX, VOCs, and VOC/NO<sub>2</sub>) at the 9 photochemical stations over South Korea since 2007 in terms of the four MEK land-use types. The values (O<sub>3</sub>, NO<sub>2</sub>, VOCs, and VOC/NO<sub>2</sub>) in the bar graph in the figure were shown in the colors of orange, blue, grey and red, respectively. The OX values were given with the symbol 'diamond' in green. The OX value, composed of NO<sub>2</sub>-independent and NO<sub>2</sub>-dependent parts, was utilized in order to understand the regional background O<sub>3</sub> concentration (i.e., the NO<sub>2</sub>-independent one) (Mazzeo et al., 2005; Han et al., 2011). According to their studies, the OX values did not necessarily

correlate to the levels of local primary pollution (i.e.,  $\text{NO}_x$ -dependent). The residence values of the  $\text{NO}_2$  and VOCs were 3-4 times greater than the greenbelt values. The  $\text{NO}_2$  (ppb) concentrations in the four land-use types were estimated to be in the following order: Commerce (C; 35.5) > Residence (R; 31.8) > Industry (I; 19.7) > Greenbelt (G; 9.9). The VOCs (ppbC) order was C (308.3) > I (199.6) > R (112.2) > G (31.2). Therefore, the anthropogenic sources of the VOC pollutants in the commerce and industry areas were likely to be more dominant than the natural ones. Nguyen et al. (2009) also reported the relative abundance of anthropogenic VOCs emissions compared to natural ones at a site in Seoul in 2004. The VOC order in the residence and commerce areas was different from  $\text{NO}_2$  order, probably due to the different anthropogenic sources for the two different pollutants. On the other hand, the greenbelt and industry  $\text{O}_3$  averages were greater than the residence and commerce ones by approximately 50%. The order for  $\text{O}_3$  (ppb) was G (35.3) > I (31.0) > C  $\approx$  R (21.8-22.0), which was almost opposite to the  $\text{NO}_2$  case.

The ratio values of the  $\text{VOC}/\text{NO}_2$  (3.6-8.7) in the residence, greenbelt, and commerce areas were generally smaller than the threshold values, while the ratio in the industry was the largest (10.2) of the four types (Table 11 and Fig. 13). The order for the ratio was I (10.2) > C (8.7) > G (3.9) > R (3.6). Therefore, the 8 stations except for the industry area among the 9 photochemical stations belonged to the VOCs-limited range which was defined as having the ratio value of less than 8 to 10 (see also Larsen et al., 2003). The industry station corresponded to the  $\text{NO}_x$ -limited chemistry. Higher  $\text{O}_3$  levels on weekends (except in industry) could be associated with lower  $\text{NO}_2$  values on weekends under the VOCs-limited  $\text{O}_3$  formation regime. This tendency was also shown in the greenbelt as well as in the residence and commerce areas, although not as evident as the residence and commerce. This result was similar to the analysis of Marr and Harley (2002b) in California. They found that a shift in  $\text{O}_3$  formation from  $\text{NO}_x$ -limited to VOCs-limited condition in the region could result from the reduction of VOCs more than that of  $\text{NO}_x$ . Based on the number of individual land-use type stations and their distribution over South Korea (Fig. 1), the VOCs control strategy for the  $\text{O}_3$  reduction in this country was overall more effective than the  $\text{NO}_x$  control strategy. However, since the sample number of the photochemical stations in this study was limited particularly in the commerce and industry areas, the strategy could be shifted with the land-use types and more photochemical station data were needed for a more rigorous result. On the other hand, the VOCs-limited condition was also shown in Shanghai, China (Tie et al., 2013).

On the other hand, according to the one-dimensional photochemical study of Liu et al. (2012) in Beijing, China, the reduction of either NO<sub>2</sub> or VOCs could induce the decrease of O<sub>3</sub> production in the transition regime from VOCs-limited to NO<sub>x</sub>-limited, which was more pronounced in the PBL. Lower VOCs in greenbelt areas than other land-use types in Fig. 10 indicate a weak contribution of the anthropogenic VOCs in greenbelt areas. Therefore the competing role between biogenic- and anthropogenic sources highly depends on the location and conditions.

The OX values ranged from a minimum (45.4 ppb) in the greenbelt areas to a maximum (57.4 ppb) in the commerce area, indicating less variability than the other pollutant values (O<sub>3</sub>, NO<sub>2</sub>, and VOCs) (Fig. 13 and Table 11). This result agreed with the analysis of Mazzeo et al. (2005) at a green area of Argentina. The OX values in some areas in Taiwan were almost constant in previous studies (Chen et al., 2002; Chou et al., 2006). This result suggested that the ‘NO<sub>x</sub>-titration’ effect (e.g., Chou et al., 2006) was an important mechanism for the O<sub>3</sub> change. The temporal O<sub>3</sub> levels in the SMA and some inland areas were lower than those in the greenbelt and coastal areas due to NO<sub>x</sub> titration effect (Kuttler and Strassburger, 1999; Ghim and Chang, 2002; Seo et al., 2014). The titration could have occurred locally even during nighttime without photochemistry from the nitrate formation and dry deposition by anthropogenic precursor emissions, and the higher O<sub>3</sub> values in the greenbelts related to the lower titration and the lower oxidization of NO (i.e., dilution) during the transport (Seo et al., 2014). Since local sources of both anthropogenic and biogenic hydrocarbons affected the oxidation (Kuttler and Strassburger, 1999; Clapp and Jenkin, 2001), their share needs to be further examined using, for instance, VOCs. Thus, O<sub>3</sub> formation in its weekly cycle could increase during weekend despite the reduced total (i.e., anthropogenic+natural) VOCs, because of their different species (Marr and Harley, 2002b).

## 9. Conclusion

We have comprehensively investigated the spatiotemporal variations in the surface air pollutants (O<sub>3</sub>, NO<sub>2</sub>, SO<sub>2</sub>, CO, and PM<sub>10</sub>) with the MEK four land-use types of residence, commerce, industry and greenbelt over South Korea from 2002 to 2013, using routinely observed hourly data at 283 stations. The variations were analyzed in terms of the cycles (diurnal, weekly, and annual) of the pollutants, their trends and inter-relationship. The VOCs

data at 9 photochemical stations available since 2007 were also utilized in order to examine their effects on the ozone chemistry. The CNSP pollutants were overall larger in a  $0.1^\circ \times 0.1^\circ$  grid (i.e., more urban characteristics), while the  $O_3$  values were larger in a  $0.25^\circ \times 0.25^\circ$  grid (i.e., more suburban/rural). The land-use types were generally consistent with the satellite-derived land covers and with the previous result (Kuttler and Strassburger, 1999) of an anti-correlation between the  $O_3$  and  $NO_2$  in diverse city areas. The relationship between the two pollutants in the SMA residence areas was substantially different from that outside of the SMA, probably due to the local difference in the vehicle emissions.

The highest concentrations of air pollutants in the cycles were found in the industrial areas for  $SO_2$  and  $PM_{10}$ , in the commercial areas for  $NO_2$  and CO and in the greenbelt areas for  $O_3$ , respectively. The CNSP pollutants, except for  $O_3$ , were generally higher in the big cities during the weekdays while the  $O_3$  showed its highest values in the small cities during the weekends. The weekly cycle and trends of the  $O_3$  were out of phase with those of the  $NO_2$ , particularly in the residential and commercial areas. Regardless of the land-use types, the CNSP pollutants had significantly decreasing trends in contrast with the  $O_3$  uptrend, probably due to the effective government controls (Kim and Shon, 2011).

The weekly cycles of the pollutants were locally sensitive to the land-use types, while their long-term trends were most commonly similar to the types and regional areas. Total oxidant values (OX) with the land-use types were analyzed for the local and regional (or background) contributions of  $O_3$ , and the OX (ppb) order was  $C (57.4) > R (53.6) > I (50.7) > G (45.4)$ , emphasizing the importance of the local part. However, the elevated  $O_3$  over South Korea in the short-term could be due to both local anthropogenic precursors ( $NO_x$  and VOCs, etc) and their transport from China (Seo et al., 2014). In addition, the local wind could affect the ozone level over the SMA and Seoul (Ghim and Chang, 2000). The values of the VOC/ $NO_2$  ratio for each of land-use types turned out to be in the order of  $I (10.2) > C (8.7) > G (3.9) > R (3.6)$ , which suggested that most of the areas (~70 %) in South Korea have to be under VOCs-limited sensitivities for ozone chemistry.

Complete observations of the pollutants from intensive field campaigns and their monitoring are required in the future together with their profile measurements (e.g., Han et al., 2009) for their reduction. In view of the  $O_3$  control, the inter-relationships between the pollutants ( $O_3$ ,  $NO_x$ , VOCs,  $PM_{10}$ , and CO) and their seasonal washout and vertical mixing have to be further investigated. The regional transport of the pollutants from China (e.g., Kim

et al., 2012), accurate assessment on their emission inventories, the meteorological condition (temperature, cloud and aerosol, air masses, etc) on the pollutants, and the relative impact of anthropogenic and biogenic VOCs on O<sub>3</sub> chemistry are beyond the scope of this study, but they need to be studied in the future.

## **Acknowledgements**

This study was supported by the National Research Foundation of Korea (NRF) grant funded by the Korean Government (MSIP) (NO. 2009-0083527) and the Korean Ministry of Environment as the Eco-technopia 21 project (NO. 201200016003).

## **References**

- Ahrens, C. D., : *Meteorology today; An Introduction to Weather, Climate, and the Environment*, 8th ed., Thomson Brooks/Cole, Belmont, California, USA, 2007.
- Anthwal, A., Park, C., Jung, K., Kim, M., and Kim, K.: The temporal and spatial distribution of volatile organic compounds (VOCs) in the urban residential atmosphere of Seoul, Korea, *Asian J. Atmos. Environ.*, 4, 42-54, 2010.
- Atkinson-Palombo, C. M., Miller, J. A., and Balling Jr, R. C.: Quantifying the ozone “weekend effect” at various locations in Phoenix, Arizona, *Atmos. Environ.*, 40, 7644-7658, 2006.
- Beirle, S., Platt, U., Wenig, M., and Wagner, T.: Weekly cycle of NO<sub>2</sub> by GOME measurements: a signature of anthropogenic sources, *Atmos. Chem. Phys.*, 3, 2225-2232, 2003.
- Bian, H., Han, S., Tie, X., Sun, M., and Liu, A.: Evidence of impact of aerosols on surface ozone concentration in Tianjin, China, *Atmos. Environ.*, 41, 4672-4681, 2007.
- Brönnimann, S., Schuepbach, E., Zanis, P., Buchmann, B., and Wanner, H.: A climatology of regional background ozone at different elevations in Switzerland (1992–1998), *Atmos. Environ.*, 34, 5191-5198, 2000.
- Chen, C., Tsuang, B., Tu, C., Cheng, W., and Lin, M.: Wintertime vertical profiles of air pollutants over a suburban area in central Taiwan, *Atmos. Environ.*, 36, 2049-2059, 2002.

Chen, L. W. A, Doddridge, B. G., Dickerson, R. R., Chow, J. C., Mueller, P. K., Quinn, J., and Butler, W. A.: Seasonal variations in elemental carbon aerosol, carbon monoxide and sulfur dioxide: Implications for sources, *Geophys. Res. Lett.*, 28, 1711-1714, 2001.

Choi, Y. S., Ho, C. H., Chen, D., Noh, Y. H., and Song, C. K.: Spectral analysis of weekly variation in PM<sub>10</sub> mass concentration and meteorological conditions over China, *Atmos. Environ.*, 42, 655-666, 2008.

Chou, C. C., Liu, S. C., Lin, C., Shiu, C., and Chang, K.: The trend of surface ozone in Taipei, Taiwan, and its causes: Implications for ozone control strategies, *Atmos. Environ.*, 40, 3898-3908, 2006.

Clapp, L. J. and Jenkin, M. E.: Analysis of the relationship between ambient levels of O<sub>3</sub>, NO<sub>2</sub> and NO as a function of NO<sub>x</sub> in the UK, *Atmos. Environ.*, 35, 6391-6405, 2001.

Cooper, O., Parrish, D., Stohl, A., Trainer, M., Nédélec, P., Thouret, V., Cammas, J., Oltmans, S., Johnson, B., and Tarasick, D.: Increasing springtime ozone mixing ratios in the free troposphere over western North America, *Nature*, 463, 344-348, 2010.

De Fries, R., Hansen, M., Townshend, J., and Sohlberg, R.: Global land cover classifications at 8 km spatial resolution: the use of training data derived from Landsat imagery in decision tree classifiers, *Int. J. Remote Sens.*, 19, 3141-3168, 1998.

Derwent, R., Jenkin, M., Saunders, S., Pilling, M., Simmonds, P., Passant, N., Dollard, G., Dumitrescu, P., and Kent, A.: Photochemical ozone formation in north west Europe and its control, *Atmos. Environ.*, 37, 1983-1991, 2003.

Diaz-de-Quijano, M., Penuelas, J., and Ribas, A.: Increasing interannual and altitudinal ozone mixing ratios in the Catalan Pyrenees, *Atmos. Environ.*, 43 (38), 6049-6057, <http://dx.doi.org/10.1016/j.atmosenv.2009.08.035m>, 2009.

Elbir, T., Kara, M., Bayram, A., Altiok, H., and Dumanoglu, Y.: Comparison of predicted and observed PM<sub>10</sub> concentrations in several urban street canyons, *Air Qual. Atmos. Health*, 4, 121-131, <http://dx.doi.org/10.1007/s11869-010-0080-9>, 2011.

Flemming, J., Stern, R., and Yamartino, R. J.: A new air quality regime classification scheme for O<sub>3</sub>, NO<sub>2</sub>, SO<sub>2</sub> and PM<sub>10</sub> observations sites, *Atmos. Environ.*, 39, 6121-6129, 2005.

Friedl, M. A., Sulla-Menashe, D., Tan, B., Schneider, A., Ramankutty, N., Sibley, A., and Huang, X.: MODIS Collection 5 global land cover: Algorithm refinements and characterization of new datasets, *Remote Sens. Environ.*, 114, 168-182, 2010.

Fujita, E. M., Stockwell, W. R., Campbell, D. E., Keislar, R. E., and Lawson D. R.: Evolution of the magnitude and spatial extent of the weekend ozone effect in California's south coast air basin, 1981-2000, *J. Air Waste Manage. Assoc.*, 53, 802-815, 2003a.

Fujita, E. M., Campbell, D. E., Zielinska, B., Sagebiel, J. C., Bowen, J. L., Goliff, W. S., Stockwell, W. R., and Lawson D. R.: Diurnal and weekday variations in the source

contributions of ozone precursors in California's south coast air basin, *J. Air Waste Manage. Assoc.*, 53, 844-863, 2003b.

Ghim, Y. S. and Chang, Y.: Characteristics of ground-level ozone distributions in Korea for the period of 1990-1995, *J. Geophys. Res. Atmos.*, 105, 8877-8890, 2000.

Gilge, S., Plass-Dülmer, C., Fricke, W., Kaiser, A., Ries, L., Buchmann, B., and Steinbacher, M.: Ozone, carbon monoxide and nitrogen oxides time series at four alpine GAW mountain stations in central Europe, *Atmos. Chem. Phys.*, 10, 12295-12316, 2010.

Han, S., Bian, H., Tie, X., Xie, Y., Sun, M., and Liu, A.: Impact of nocturnal planetary boundary layer on urban air pollutants: Measurements from a 250-m tower over Tianjin, China, *J. Hazard. Mater.*, 162, 264-269, 2009.

Han, S., Bian, H., Feng, Y., Liu, A., Li, X., Zeng, F., and Zhang, X.: Analysis of the relationship between O<sub>3</sub>, NO and NO<sub>2</sub> in Tianjin, China, *Aerosol Air Qual. Res.*, 11, 128-139, 2011.

Hansen, M., DeFries, R., Townshend, J. R., and Sohlberg, R.: Global land cover classification at 1 km spatial resolution using a classification tree approach, *Int. J. Remote Sens.*, 21, 1331-1364, 2000.

He, H., Li, C., Loughner, C. P., Li, Z., Krotkov, N. A., Yang, K., Wang, L., Zheng, Y., Bao, X., Zhao, G., Dickerson, R. R.: SO<sub>2</sub> over central China: Measurements, numerical simulations and the tropospheric sulfur budget, *J. Geophys. Res.*, 117, D00K37, doi:10.1029/2011JD016473, 2012.

Jacobson, M. Z.: *Atmospheric Pollution: History, Science, and Regulation*, Cambridge University Press, Cambridge, United Kingdom, 2002.

Jin, L., Lee, S.-H., Shin, H.-J., and Kim, Y. P.: A Study on the Ozone Control Strategy using the OZIPR in the Seoul Metropolitan Area, *Asian J. Atmos. Environ.*, 6, 111-117, 2012.

Kaiser, A., Scheifinger, H., Spangl, W., Weiss, A., Gilge, S., Fricke, W., Ries, L., Cemas, D., and Jesenovec, B.: Transport of nitrogen oxides, carbon monoxide and ozone to the alpine global atmosphere watch stations Jungfraujoch (Switzerland), Zugspitze and Hohenpeißenberg (Germany), Sonnblick (Austria) and Mt. Krvavec (Slovenia), *Atmos. Environ.*, 41, 9273-9287, 2007.

Klemm, O., Stockwell, W. R., Schlager, H., and Krautstrunk, M.: NO<sub>x</sub> or VOC limitation in East German ozone plumes?, *J. Atmos. Chem.*, 25, 1-18, 2000.

Kim, J. Y., Kim, S., Ghim, Y. S., Song, C. H., and Yoon, S.: Aerosol properties at Gosan in Korea during two pollution episodes caused by contrasting weather conditions, *Asia Pac. J. Atmos. Sci.*, 48, 25-33, 2012.

Kim, K. and Shon, Z.: Long-term changes in PM<sub>10</sub> levels in urban air in relation with air quality control efforts, *Atmos. Environ.*, 45, 3309-3317, 2011.

Kim, N. K., Kim, Y. P., and Kang, C.-H.: Long-term trend of aerosol composition and direct radiative forcing due to aerosols over Gosan: TSP, PM<sub>10</sub>, and PM<sub>2.5</sub> data between 1992 and 2008, *Atmos. Environ.*, 45, 6107-6115, 2011.

Kim, N. K., Kim, Y. P., Morino, Y., Kurokawa, J., and Ohara, T.: Verification of NO<sub>x</sub> emission inventory over South Korea using sectoral activity data and satellite observation of NO<sub>2</sub> vertical column densities, *Atmos. Environ.*, 77, 496-508, 2013a.

Kim, S., Lee, M., Kim, S., Choi, S., Seok, S., and Kim, S.: Photochemical characteristics of high and low ozone episodes observed in the Taehwa Forest observatory (TFO) in June 2011 near Seoul South Korea, *Asia Pac. J. Atmos. Sci.*, 49, 325-331, 2013b.

Kim, S. W., Heckel, A., McKeen, S., Frost, G., Hsie, E., Trainer, M., Richter, A., Burrows, J., Peckham, S., and Grell, G.: Satellite-observed US power plant NO<sub>x</sub> emission reductions and their impact on air quality, *Geophys. Res. Lett.*, 33, L22812, doi:10.1029/2006GL027749, 2006.

Kuttler, W. and Strassburger, A.: Air quality measurements in urban green areas—a case study, *Atmos. Environ.*, 33, 4101-4108, 1999.

Lal, S., Naja, M., and Subbaraya, B. H.: Seasonal variations in surface ozone and its precursors over an urban site in India, *Atmos. Environ.*, 34, 2713-2724, 2000.

Lamsal, L., Martin, R., Padmanabhan, A., van Donkelaar, A., Zhang, Q., Sioris, C., Chance, K., Kurosu, T., and Newchurch, M.: Application of satellite observations for timely updates to global anthropogenic NO<sub>x</sub> emission inventories, *Geophys. Res. Lett.*, 38, L05810, doi:10.1029/2010GL046476, 2011.

Lamsal, L., Martin, R., van Donkelaar, A., Celarier, E., Bucsela, E., Boersma, K., Dirksen, R., Luo, C., and Wang, Y.: Indirect validation of tropospheric nitrogen dioxide retrieved from the OMI satellite instrument: Insight into the seasonal variation of nitrogen oxides at northern midlatitudes, *J. Geophys. Res. Atmos.*, 115, D05302, doi:10.1029/2009JD013351, 2010.

Larsen, L. C., Austin, J., Dolislager, L., Lashgari, A., McCauley, E., Motallebi, N., and Tran, H.: The ozone weekend effect in California, California Environment of Protection Agency, Sacramento, California, USA, 2003.

Lee, H., Kim, S., Brioude, J., Cooper, O., Frost, G., Kim, C., Park, R., Trainer, M., and Woo, J.: Transport of NO<sub>x</sub> in East Asia identified by satellite and in situ measurements and Lagrangian particle dispersion model simulations, *J. Geophys. Res. Atmos.*, 119, 2574-2596, doi:10.1002/2013JD021185, 2014.

Lee, Y.-R., Yoo, J.-M., Jeong, M.-J., Won, Y.-I., Hearty, T., and Shin, D.-B.: Comparison between MODIS and AIRS/AMSU satellite-derived surface skin temperatures. *Atmos. Meas. Tech.* 6, 445-455, 2013.



- Levy, H., II, Moxim, W. J., Klonecki, A. A., and Kasibhatla, P. S.: Simulated tropospheric NO<sub>x</sub>: Its evaluation, global distribution and individual source contributions, *J. Geophys. Res.*, 104, 26279–26306, 1999.
- Li, C., Krotkov, N. A., Dickerson, R. R., Li, Z., Yang, K., and Chin, M.: Transport and evolution of a pollution plume from northern China: A satellite-based case study, *J. Geophys. Res.*, 115, D00K03, doi:10.1029/2009JD012245, 2010.
- Liu, Z., Wang, Y., Gu, D., Zhao, C., Huey, L., Stickel, R., Liao, J., Shao, M., Zhu, T., and Zeng, L.: Summertime photochemistry during CAREBeijing-2007, RO<sub>x</sub> budgets and O<sub>3</sub> formation, *Atmos. Chem. Phys.*, 12, 7737-7752, 2012.
- Marr, L. C. and Harley, R. A.: Modeling the effect of weekday-weekend differences in motor vehicle emissions on photochemical air pollution in central California, *Environ. Sci. Technol.*, 36, 4099-4106, 2002a.
- Marr, L. C. and Harley, R. A.: Spectral analysis of weekday-weekend differences in ambient ozone, nitrogen oxide, and non-methane hydrocarbon time series in California, *Atmos. Environ.*, 36, 2327-2335, 2002b.
- Masiol, M., Agostinelli, C., Formenton, G., Tarabotti, E., and Pavoni, B.: Thirteen years of air pollution hourly monitoring in a large city: Potential sources, trends, cycles and effects of car-free days, *Sci. Total Environ.*, 494-495, 84-96, doi: 10.1016/j.scitotenv.2014.06.122, 2014.
- Mayer, H.: Air pollution in cities, *Atmos. Environ.*, 33, 4029-4037, 1999.
- Mazzeo, N. A., Venegas, L. E., and Choren, H.: Analysis of NO, NO<sub>2</sub>, O<sub>3</sub> and NO<sub>x</sub> concentrations measured at a green area of Buenos Aires City during wintertime, *Atmos. Environ.*, 39, 3055-3068, 2005.
- Meng, Z., Xu, X., Yan, P., Ding, G., Tang, J., Lin, W., Xu, X., and Wang, S.: Characteristics of trace gaseous pollutants at a regional background station in Northern China, *Atmos. Chem. Phys.*, 9, 927-936, 2009.
- Mijling, B., van der A. R., and Zhang, Q.: Regional nitrogen oxides emission trends in East Asia observed from space, *Atmos. Chem. Phys.*, 13, 12003-12012, 2013.
- Nevers, N.D.: *Air Pollution Control Engineering*, 2<sup>nd</sup> ed., McGraw-Hill Companies, Inc., New York, 571-573, 2000.
- Nguyen, H. T., Kim, K., and Kim, M.: Volatile organic compounds at an urban monitoring station in Korea, *J. Hazard. Mater.*, 161, 163-174, 2009.
- NIER: Regulation on Type Approval Certificate and Performance Test of Environmental Instrument (<http://www.law.go.kr/>), Ordinance of Ministry of Environment, Seoul, Korea, (last access: July 31 2015), 2010.

- Novelli, P. C., Masarie, K. A., Lang, P. M., Hall, B. D., Myers, R. C., and Elkins, J. W.: Reanalysis of tropospheric CO trends: Effects of the 1997-1998 wildfires, *J. Geophys. Res.*, 108(D15), 4464, doi:10.1029/2002JD003031, 2003.
- Oh, I., Kim, Y., and Kim, C.: An observational and numerical study of the effects of the late sea breeze on ozone distributions in the Busan metropolitan area, Korea, *Atmos. Environ.*, 40, 1284-1298, 2006.
- Pandey Deolal, S., Brunner, D., Steinbacher, M., Weers, U., and Staehelin, J.: Long-term in situ measurements of NO<sub>x</sub> and NO<sub>y</sub> at Jungfraujoch 1998–2009: time series analysis and evaluation, *Atmos. Chem. Phys.*, 12, 2551-2566, 2012.
- Pochanart, P., Hirokawa, J., Kajii, Y., Akimoto, H., and Nakao, M.: Influence of regional-scale anthropogenic activity in northeast Asia on seasonal variations of surface ozone and carbon monoxide observed at Oki, Japan, *J. Geophys. Res. Atmos.*, 104, 3621-3631, 1999.
- Pudasainee, D., Sapkota, B., Shrestha, M. L., Kaga, A., Kondo, A., and Inoue, Y.: Ground level ozone concentrations and its association with NO<sub>x</sub> and meteorological parameters in Kathmandu valley, Nepal, *Atmos. Environ.*, 40, 8081-8087, 2006.
- Qin, Y., Tonnesen, G., and Wang, Z.: One-hour and eight-hour average ozone in the California South Coast air quality management district: trends in peak values and sensitivity to precursors, *Atmos. Environ.*, 38, 2197-2207, 2004a.
- Qin, Y., Tonnesen, G., and Wang, Z.: Weekend/weekday differences of ozone, NO<sub>x</sub>, CO, VOCs, PM<sub>10</sub> and the light scatter during ozone season in southern California, *Atmos. Environ.*, 38, 3069-3087, 2004b.
- Sakamoto, M., Yoshimura, A., Kosaka, H., and Hiraki, T.: Study on weekend–weekday differences in ambient oxidant concentrations in Hyogo prefecture, *J. Japan Soc. Atmos. Environ.*, 40, 201-208, 2005.
- Sarangi, T., Naja, M., Ojha, N., Kumar, R., Lal, S., Venkataramani, S., Kumar, A., Sagar, R., and Chandola, H. C.: First simultaneous measurements of ozone, CO, and NO<sub>y</sub> at a high-altitude regional representative site in the central Himalayas, *J. Geophys. Res. Atmos.*, 119, 1592-1611, doi:10.1002/2013JD020631, 2014.
- Seinfeld, J. H. and Pandis, S. N.: *Atmospheric Chemistry and Physics-From Air Pollution to Climate Change*, John Wiley & Sons, New Jersey, 2006.
- Seo, J., Youn, D., Kim, J., and Lee, H.: Extensive spatiotemporal analyses of surface ozone and related meteorological variables in South Korea for the period 1999–2010, *Atmos. Chem. Phys.*, 14, 6395-6415, 2014.
- Sharma, A. P., Kim, K., Ahn, J., Shon, Z., Sohn, J., Lee, J., Ma, C., and Brown, R. J.: Ambient particulate matter (PM<sub>10</sub>) concentrations in major urban areas of Korea during 1996-2010., *Atmospheric Pollution Research*, 5, 161-169, doi:10.5094/APR.2014.020, 2014.

- Shon, Z. and Kim, K.: Impact of emission control strategy on NO<sub>2</sub> in urban areas of Korea, *Atmos. Environ.*, 45, 808-812, 2011.
- Stockwell, W. and Calvert, J. G.: The mechanism of the HO-SO<sub>2</sub> reaction, *Atmos. Environ.*, 17, 11, 2231-2235, 1983.
- Tie, X., Geng, F., Guenther, A., Cao, J., Greenberg, J., Zhang, R., Apel, E., Li, G., Weinheimer, A., and Chen, J.: Megacity impacts on regional ozone formation: observations and WRF-Chem modeling for the MIRAGE-Shanghai field campaign, *Atmos. Chem. Phys.*, 13, 5655-5669, 2013.
- Ulke, A. G. and Mazzeo, N. A.: Climatological aspects of the daytime mixing height in Buenos Aires city, Argentina. *Atmos. Environ.*, 32, 1615–1622, 1998.
- Valks, P., Pinardi, G., Richter, A., Lambert, J., Hao, N., Loyola, D., van Roozendaal, M., and Emmadi, S.: Operational total and tropospheric NO<sub>2</sub> column retrieval for GOME-2, *Atmos. Meas. Tech.*, 4, 1491-1514, 2011.
- Wang, T., Cheung, V. T., Anson, M., and Li, Y.: Ozone and related gaseous pollutants in the boundary layer of eastern China: Overview of the recent measurements at a rural site, *Geophys. Res. Lett.*, 28, 2373-2376, 2001.
- Wang, W. X. and Wang, T.: On the origin and the trend of acid rain precipitation in China, *Water Air Soil Poll.*, 85, 2295-2300, 1995.
- Wang, Y., Konopka, P., Liu, Y., Chen, H., Müller, R., Plöger, F., Riese, M., Cai, Z., and Lü, D.: Tropospheric ozone trend over Beijing from 2002–2010: ozonesonde measurements and modeling analysis, *Atmos. Chem. Phys.*, 12, 8389-8399, 2012.
- Wang, Y., Zhang, Q., He, K., Zhang, Q., and Chai, L.: Sulfate-nitrate-ammonium aerosols over China: response to 2000–2015 emission changes of sulfur dioxide, nitrogen oxides, and ammonia, *Atmos. Chem. Phys.*, 13, 2635-2652, 2013.
- Wang, Y., McElroy, M. B., Munger, J. W., Hao, J., Ma, H., Nielsen, C., and Chen, Y.: Variations of O<sub>3</sub> and CO in summertime at a rural site near Beijing, *Atmos. Chem. Phys.*, 8, 6355-6363, 2008.
- Wilks, D. S.: *Statistical Methods in the Atmospheric Sciences*, Academic Press, San Diego, California, USA, 1995. WMO, WMO Global Atmosphere Watch (GAW) Strategic Plan (2008-2015), GAW Report No. 172 (WMO TD NO. 1384), World Meteorological Organization, Geneva, Switzerland, <http://gaw.empa.ch/gawsis>, (last access: May 4 2015), 2007.
- Xu, X., Lin, W., Wang, T., Yan, P., Tang, J., Meng, Z., and Wang, Y.: Long-term trend of surface ozone at a regional background station in eastern China 1991–2006: enhanced variability, *Atmos. Chem. Phys.*, 8, 2595-2607, 2008.

Yoo, J.-M., Lee, Y.-R., Kim, D.-C., Oh, S.-M., Jeong, M.-J., Stockwell, W., Kundu, P., Shin, D. -B., and Lee, S. -J.: New indices for wet scavenging of air pollutants (O<sub>3</sub>, CO, NO<sub>2</sub>, SO<sub>2</sub> and PM<sub>10</sub>) by summertime rain. *Atmos. Environ.*, 82, 226-237, 2014.

Zhang, Q., Streets, D. G., and He, K.: Satellite observations of recent power plant construction in Inner Mongolia, China, *Geophys. Res. Lett.*, 36, L15809, doi:10.1029/2009GL038984, 2009.

Table 1. List of acronyms used in this study.

Acronyms	Original words	Details
R	Residence	Residential Areas : Areas necessary to protect peaceful dwelling and sound living environment
C	Commerce	Commercial Areas : Areas necessary to increase convenience in commerce and other businesses
I	Industry	Industrial Areas : Areas necessary to increase convenience of industries
G	Greenbelt	Green Areas : Areas requiring the conservation of green areas to protect the natural environment, farmland and forests, health and sanitation, security and to prevent any disorderly sprawl of cities
SMA	Seoul Metropolitan Area	
CNSP	CO, NO <sub>2</sub> , SO <sub>2</sub> and PM <sub>10</sub>	
OZIPR	Ozone Isopleth Plotting Package for Research	
MEK	Ministry of Environment of Korea	
MLIT	Ministry of Land, Infrastructure and Transport	
AVHRR	Advanced Very High Resolution Radiometer	
MODIS	Moderate-resolution Imaging Spectroradiometer	

Table 2. Data information of the surface air pollutants (O<sub>3</sub>, CO, NO<sub>2</sub>, SO<sub>2</sub> and PM<sub>10</sub>) measured at 283 air pollution monitoring stations of the Ministry of Environment of Korea (MEK) in South Korea during 2002-2013. The information for the VOCs at 9 of the photochemical MEK stations, simultaneously measured with the other pollutants at the same sites, has also been shown. The 9 out of the total 19 VOCs stations were selected in this study, based on their locations and their relatively long-term records since 2007.

Air pollutant	Source	Period	Time interval	Number of stations				
				Residence	Commerce	Industry	Greenbelt	Total
O <sub>3</sub> , CO, NO <sub>2</sub> , SO <sub>2</sub> , PM <sub>10</sub>	MEK	Jan 2002 – Dec 2013	Hourly	154	57	35	37	283
VOCs	MEK	Jan 2007 – Dec 2013	Hourly	3	1	0	3	7
VOCs at Daemyoung (128.57E, 35.84N)	MEK	Jan 2010 – Dec 2013	Hourly	1	0	0	0	1
VOCs at Joongheung (126.68E, 34.83N)	MEK	Jan 2008 – Dec 2013	Hourly	0	0	1	0	1

Table 3. Methods and instruments for measuring the surface air pollutants (O<sub>3</sub>, CO, NO<sub>2</sub>, SO<sub>2</sub> and PM<sub>10</sub>) at 283 MEK air pollution monitoring stations in South Korea during 2002-2013.

Air Pollutant	Method	Instrument
O <sub>3</sub>	U.V Photometric Method	Thermo, 49i
CO	Non-Dispersive Infrared Method	Thermo, 48CTL
NO <sub>2</sub>	Chemiluminescent Method	Thermo, 42CTL
SO <sub>2</sub>	Pulse U.V Fluorescence Method	Thermo, 43CTL
PM <sub>10</sub>	β-ray Absorption Method	Thermo, FH62-C14
VOC	TD-GC/MS (Thermal Desorption Gas Chromatography/Mass Spectrometry)	Agilent, Perkinelmer, Varian

Table 4. Comparison of the four land-use types of the MEK (residence, commerce, industry, and greenbelt) for 283 air pollution monitoring stations of the MEK during 2002-2012 with the satellite-derived land-cover types of the AVHRR and MODIS in a 0.25° x 0.25° grid. The AVHRR data were available for 13 land-cover types over the globe at a 1km x 1km pixel resolution during 1981-1994 (e.g., De Fries et al., 1998; Hansen et al., 2000). The MODIS data have been derived for 17 land-cover types over the globe at a 5km x 5km spatial resolution during 2002-2012 (e.g., Friedl et al., 2010). In this study, for comparison, the AVHRR and MODIS original types were regrouped into the following four land-cover types: forest/wood, grass/shrub, urban/built-up and water. In the table, the values with and without parentheses indicate the MODIS and AVHRR data, respectively.

Land Cover	Residence (%)	Commerce (%)	Industry (%)	Greenbelt (%)
Forest/Wood	12.4 (31.8)	15.8 (35.8)	8.6 (26.2)	35.2 (37.2)
Grass/Shrub	58.4 (27.5)	43.9 (18.0)	60.0 (19.2)	43.2 (21.8)
Urban/Built-up	19.5 (28.8)	33.3 (32.2)	11.4 (28.6)	0.0 (16.4)
Water	9.7 (11.9)	7.0 (14.0)	20.0 (26.0)	21.6 (24.6)

Table 5. Climatological averages of (a) O<sub>3</sub> (ppb), (b) CO (0.1 ppm), (c) NO<sub>2</sub> (ppb), (d) SO<sub>2</sub> (ppb), and (e) PM<sub>10</sub> (μgm<sup>-3</sup>) in two types of spatial grids (0.25°×0.25° and 0.1°×0.1°) over South Korea during 2002-2013. The standard deviation (σ) values of the five kinds of variables are also presented with the ± values.

	Spring	Summer	Fall	Winter	Annual
<b>&lt; 0.25°×0.25°&gt;</b>					
O <sub>3</sub> (ppb)	34.93±7.69	27.22±4.44	22.34±7.22	19.62±7.08	26.08±6.33
CO (0.1ppm)	5.38±1.12	4.16±0.92	5.41±1.24	7.23±2.05	5.53±1.23
NO <sub>2</sub> (ppb)	18.10±8.25	13.14±6.25	17.92±8.35	21.13±9.01	17.54±7.88
SO <sub>2</sub> (ppb)	4.89±1.65	3.57±1.71	4.23±1.61	6.49±2.43	4.78±1.67
PM <sub>10</sub> (μgm <sup>-3</sup> )	64.47±8.41	41.2±6.21	45.57±7.49	54.82±10.89	51.46±7.72
<b>&lt; 0.1°×0.1°&gt;</b>					
O <sub>3</sub> (ppb)	33.08±7.37	26.42±4.24	20.87±6.51	17.95±6.59	24.63±5.88
CO (0.1ppm)	5.38±1.14	4.21±0.97	5.49±1.30	7.30±2.06	5.58±1.27
NO <sub>2</sub> (ppb)	21.10±9.59	15.48±7.42	20.79±9.27	24.12±9.99	20.34±8.96
SO <sub>2</sub> (ppb)	5.27±1.97	3.97±2.10	4.60±1.86	6.82±2.45	5.15±1.90
PM <sub>10</sub> (μgm <sup>-3</sup> )	66.53±9.90	42.91±7.01	47.63±8.53	57.31±12.30	53.58±8.91

Table 6. The spatial mean and standard deviation of the surface air pollutant concentration averages (O<sub>3</sub>, CO, NO<sub>2</sub>, SO<sub>2</sub>, and PM<sub>10</sub>) in the diurnal, weekly, and annual variations over South Korea during 2002-2013 in a 0.25°×0.25° grid in terms of the four land-use types of MEK as follows: residence (R), commerce (C), industry (I), and greenbelt (G). Here the values in parentheses denote the mean and standard deviation in a 0.1°×0.1° grid.

Cycle and pollutants	Residence		Commerce		Industry		Greenbelt	
<b>Diurnal</b>								
O <sub>3</sub>	24.3±8.07	(23.5±8.19)	21.3±6.93	(20.2±6.80)	23.5±7.24	(23.5±7.20)	30.9±7.69	(30.4±7.78)
CO	5.7±0.56	(5.7±0.60)	6.2±0.63	(6.4±0.60)	5.7±0.39	(5.8±0.42)	4.6±0.26	(4.7±0.28)
NO <sub>2</sub>	21.1±3.62	(23.1±3.87)	25.1±4.19	(28.1±4.33)	23.2±3.02	(23.8±2.98)	11.7±1.52	(12.7±1.70)
SO <sub>2</sub>	5.2±0.33	(5.3±0.35)	5.6±0.39	(5.7±0.41)	6.8±0.79	(7.5±0.85)	3.3±0.23	(3.4±0.24)
PM <sub>10</sub>	52.7±3.04	(53.3±2.87)	54.0±3.37	(55.2±3.28)	56.0±2.98	(56.4±3.01)	48.4±2.20	(49.5±2.33)
<b>Weekly</b>								
O <sub>3</sub>	24.2±0.72	(23.4±0.81)	21.2±0.75	(20.2±0.84)	23.4±1.19	(23.4±1.22)	30.8±0.41	(30.3±0.46)
CO	5.7±0.01	(5.7±0.11)	6.2±0.16	(6.4±0.18)	5.7±0.14	(5.8±0.14)	4.6±0.01	(4.7±0.01)
NO <sub>2</sub>	21.1±1.32	(23.1±1.48)	25.1±1.42	(28.2±1.65)	23.2±1.99	(23.8±2.03)	11.7±0.69	(12.7±0.78)
SO <sub>2</sub>	5.2±0.15	(5.3±0.15)	5.5±0.12	(5.7±0.15)	6.8±0.29	(7.5±0.30)	3.3±0.02	(3.4±0.01)
PM <sub>10</sub>	52.7±1.19	(53.3±1.31)	54.0±1.20	(55.2±1.43)	56.1±2.25	(56.4±2.25)	48.4±0.71	(49.4±0.82)
<b>Annual</b>								
O <sub>3</sub>	24.0±6.96	(23.4±6.89)	20.9±6.25	(20.2±6.12)	23.2±6.23	(23.4±6.28)	30.7±7.35	(30.3±7.34)
CO	5.8±1.32	(5.7±1.30)	6.3±1.42	(6.4±1.36)	5.8±0.93	(5.8±0.93)	4.7±0.89	(4.7±0.92)
NO <sub>2</sub>	21.1±4.01	(23.2±4.27)	25.2±3.79	(28.2±3.91)	23.2±3.47	(23.8±3.55)	11.7±2.37	(12.8±2.59)
SO <sub>2</sub>	5.2±1.28	(5.3±1.23)	5.6±1.39	(5.7±1.31)	6.8±0.87	(7.5±0.76)	3.4±0.92	(3.4±0.93)
PM <sub>10</sub>	53.1±10.40	(53.3±10.45)	54.5±10.93	(55.2±10.83)	56.4±9.68	(56.3±9.45)	48.8±9.85	(49.6±9.82)

Table 7. The magnitude order of the surface air pollutant concentration averages (O<sub>3</sub>, CO, NO<sub>2</sub>, SO<sub>2</sub>, and PM<sub>10</sub>) in the diurnal, weekly and annual variations of Fig. 6 over South Korea during 2002-2013 in a 0.25°×0.25° grid in terms of the four land-use types of MEK as follows: residence (R), commerce (C), industry (I) and greenbelt (G). The numbers in the table indicate the ranking of each pollutant, based on the pollutant concentration values over the types. Here the greater concentration, the higher ranking. If the orders in the two grids are different from each other, then those in parentheses have been shown for the 0.1°×0.1° grid.

Cycle/pollutants	Residence	Commerce	Industry	Greenbelt	Order
<b>Diurnal</b>					
O <sub>3</sub>	2 (2)	4 (4)	3 (3)	1 (1)	G>R>I>C
CO	2 (3)	1 (1)	3 (2)	4 (4)	C>R>I>G (C>I>R>G)
NO <sub>2</sub>	3 (3)	1 (1)	2 (2)	4 (4)	C>I>R>G
SO <sub>2</sub>	3 (3)	2 (2)	1 (1)	4 (4)	I>C>R>G
PM <sub>10</sub>	3 (3)	2 (2)	1 (1)	4 (4)	I>C>R>G
<b>Weekly</b>					
O <sub>3</sub>	2 (2)	4 (4)	3 (3)	1 (1)	G>R>I>C
CO	2 (3)	1 (1)	3 (2)	4 (4)	C>R>I>G (C>I>R>G)
NO <sub>2</sub>	3 (3)	1 (1)	2 (2)	4 (4)	C>I>R>G
SO <sub>2</sub>	3 (3)	2 (2)	1 (1)	4 (4)	I>C>R>G
PM <sub>10</sub>	3 (3)	2 (2)	1 (1)	4 (4)	I>C>R>G
<b>Annual</b>					
O <sub>3</sub>	2 (2)	4 (4)	3 (3)	1 (1)	G>R>I>C
CO	2 (3)	1 (1)	3 (2)	4 (4)	C>R>I>G (C>I>R>G)
NO <sub>2</sub>	3 (3)	1 (1)	2 (2)	4 (4)	C>I>R>G
SO <sub>2</sub>	3 (3)	2 (2)	1 (1)	4 (4)	I>C>R>G
PM <sub>10</sub>	3 (3)	2 (2)	1 (1)	4 (4)	I>C>R>G

Table 8. Comparisons of the climatological annual averages over South Korea during 2002-2013, based on the two types of spatial scale analyses of the  $0.1^\circ \times 0.1^\circ$  and  $0.25^\circ \times 0.25^\circ$  grids. The  $0.1^\circ \times 0.1^\circ$  grid averages (compared to those of  $0.25^\circ \times 0.25^\circ$ ) generally tend to show the characteristics in big urban cities rather than in suburban small suburban cities, because the air-pollution monitoring stations are more densely located in the former areas.

Air pollutant	Average ( $0.1^\circ \times 0.1^\circ$ ) minus Average ( $0.25^\circ \times 0.25^\circ$ )			
	Residence	Commerce	Industry	Greenbelt
<b>O<sub>3</sub> (ppb)</b>	-0.513	-0.735	0.181	-0.342
<b>CO (0.1 ppm)</b>	-0.067	0.093	0.052	0.009
<b>NO<sub>2</sub> (ppb)</b>	2.020	2.969	0.573	0.767
<b>SO<sub>2</sub> (ppb)</b>	0.036	0.123	0.687	0.033
<b>PM<sub>10</sub> (<math>\mu\text{g m}^{-3}</math>)</b>	0.270	0.711	-0.012	0.409



Table 9. Trends of surface air pollutants (O<sub>3</sub>, NO<sub>2</sub>, OX, CO, SO<sub>2</sub> and PM<sub>10</sub>) over South Korea during 2002-2013, based on the three types of analyses (0.1°×0.1° grid and 0.25°×0.25° grid) over the four land-use types of the MEK of residence (R), commerce (C), industry (I), and greenbelt (G). The magnitude order for the trends of each of the pollutant over the types has been shown in the figures. The ± trend values indicate the 95% confidence intervals. It should be noted that the trend values are statistically significant except for some of the NO<sub>2</sub> and SO<sub>2</sub> cases, marked by an asterisk(\*).

	Residence	Commerce	Industry	Greenbelt	Trend	Order
<b>0.25°×0.25°</b>						
O <sub>3</sub> (ppb yr <sup>-1</sup> )	0.501±0.098	0.407±0.095	0.352±0.093	0.369±0.094	increase	R>C>G>I
NO <sub>2</sub> (ppb yr <sup>-1</sup> )	-0.295±0.081	-0.042±0.088*	-0.135±0.084	-0.100±0.053	decrease	R>I>G>C*
OX (ppb yr <sup>-1</sup> )	0.205±0.107	0.365±0.103	0.231±0.113	0.260±0.103	increase	C>G>I>R
CO (0.1ppm yr <sup>-1</sup> )	-0.202±0.021	-0.210±0.021	-0.247±0.025	-0.135±0.022	decrease	I>C>R>G
SO <sub>2</sub> (ppb yr <sup>-1</sup> )	-0.036±0.024	-0.114±0.028	-0.140±0.029	-0.060±0.016	decrease	I>C>G>R
PM <sub>10</sub> (μgm <sup>-3</sup> yr <sup>-1</sup> )	-1.038±0.459	-1.014±0.456	-1.003±0.480	-1.098±0.485	decrease	G>R>C>I
<b>0.1°×0.1°</b>						
O <sub>3</sub> (ppb yr <sup>-1</sup> )	0.545±0.096	0.462±0.092	0.340±0.094	0.326±0.095	increase	R>C>I>G
NO <sub>2</sub> (ppb yr <sup>-1</sup> )	-0.240±0.083	-0.078±0.092*	-0.054±0.084*	-0.023±0.054*	decrease	R>C*>I*>G*
OX (ppb yr <sup>-1</sup> )	0.304±0.108	0.396±0.106	0.299±0.110	0.300±0.102	increase	C>R>G>I
CO (0.1ppm yr <sup>-1</sup> )	-0.175±0.021	-0.204±0.020	-0.246±0.025	-0.124±0.022	decrease	I>C>R>G
SO <sub>2</sub> (ppb yr <sup>-1</sup> )	-0.019±0.023*	-0.104±0.027	-0.177±0.030	-0.050±0.015	decrease	I>C>G>R
PM <sub>10</sub> (μgm <sup>-3</sup> yr <sup>-1</sup> )	-1.374±0.535	-1.290±0.474	-0.926±0.492	-1.049±0.485	decrease	R>C>G>I

Table 10. Climatological average value of O<sub>3</sub> (ppb) and NO<sub>2</sub> (ppb) over South Korea during 2002-2013 in terms of the MEK four land-use types (residence, commerce, industry and greenbelt) over the 283 total stations and the 209 stations excluding the 74 SMA residence areas, respectively. The spatial variation in the pollutant concentrations for the individual type is presented with the standard deviation of ± values. The number in the parenthesis indicates the ranking of each pollutant, based on concentration value over the type.

Land-use type	Air Pollutant	All stations		Stations excluding the SMA residence areas	
		O <sub>3</sub>	NO <sub>2</sub>	O <sub>3</sub>	NO <sub>2</sub>
<b>&lt;Annual&gt;</b>					
Residence		22.4±4.32 (3)	25.9±8.15 (2)	25.0±4.03 (2)	20.3±4.94 (3)
Commerce		19.2±4.85 (4)	31.3±12.00 (1)		
Industry		23.4±4.32 (2)	24.3±6.89 (3)	23.4±4.32 (3)	24.3±6.89 (2)
Greenbelt		30.2±7.83 (1)	13.3±9.63 (4)		
<b>&lt;Winter only&gt;</b>					
Residence		15.4±4.91 (3)	30.6±9.04 (2)	18.3±4.80 (2)	24.4±6.00 (3)
Commerce		13.2±4.28 (4)	34.6±11.29(1)		
Industry		16.7±4.43 (2)	27.8±7.52 (3)	16.7±4.43 (3)	27.8±7.52 (2)
Greenbelt		24.4±8.72 (1)	16.3±11.27(4)		

Table 11. The spatial mean values of the long-term surface air pollutant concentration averages ( $O_3$ ,  $NO_2$ , OX, VOC, and  $VOC/NO_2$ ) at 9 of the photochemical air pollution monitoring stations of the MEK over South Korea since 2007 in terms of the four MEK land-use categories as follows: residence (R), commerce (C), industry (I), and greenbelt (G).

<b>Air pollutant</b>	<b>Residence</b>	<b>Commerce</b>	<b>Industry</b>	<b>Greenbelt</b>	<b>Average</b>
<b><math>O_3</math> (ppb)</b>	21.8±1.24	22.0	31.0	35.5±0.43	27.6
<b><math>NO_2</math> (ppb)</b>	31.8±2.18	35.5	19.7	9.9±0.39	24.2
<b>OX=<math>O_3+NO_2</math> (ppb)</b>	53.6±1.00	57.4	50.7	45.4±0.29	51.8
<b>VOC (ppbC)</b>	112.2±14.84	308.3	199.6	31.2±2.14	162.8
<b>VOC/<math>NO_2</math></b>	3.6±0.27	8.7	10.2	3.9±0.13	6.6

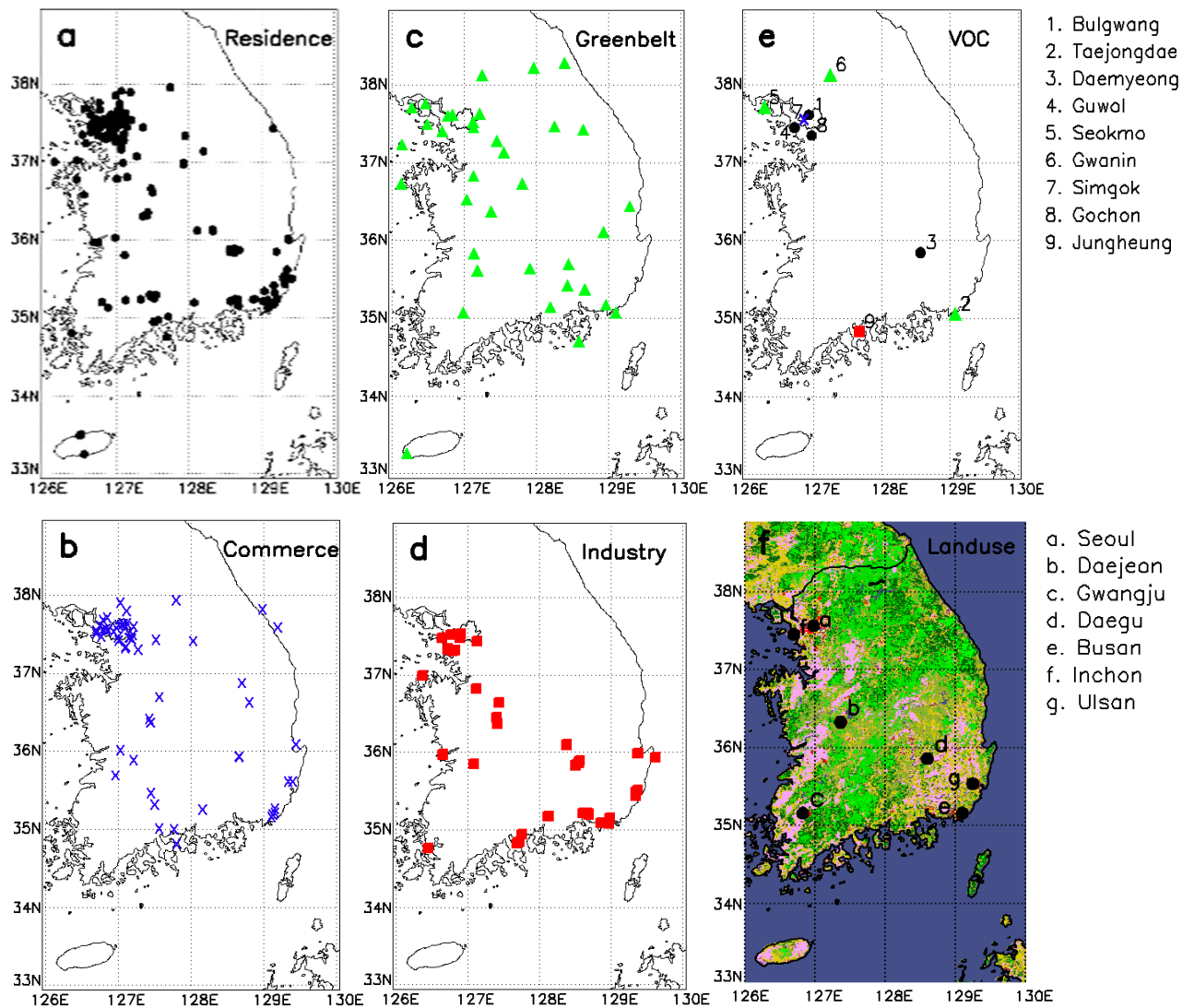


Fig. 1. Locations of surface air pollution ( $O_3$ ,  $CO$ ,  $NO_2$ ,  $SO_2$ , and  $PM_{10}$ ) monitoring stations in South Korea during 2002-2013 under the MEK four land-use types of a) residence (black circle), b) commerce (blue cross), c) greenbelt (green triangle) and d) industry (red square). e) Locations of the VOC monitoring stations, used in this study, under the four land-use types. f) Locations of seven major cities in South Korea with the satellite driven AVHRR land-cover types. The VOCs and the five kinds of air pollutants were simultaneously measured at the nine stations in Fig. 1e. Please see Table 1 for the observational periods of VOCs.

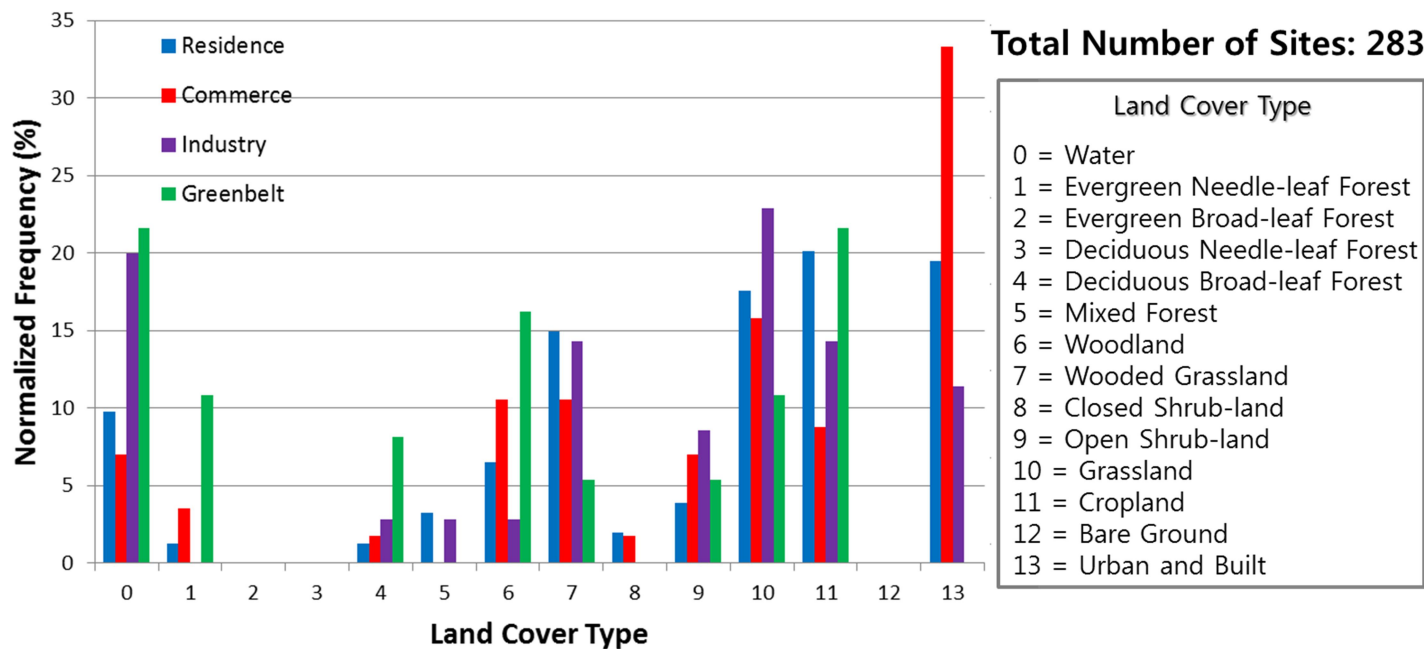


Fig. 2. Satellite-derived AVHRR land-cover types with respect to the MEK four land-use types (residence, commerce, industry and greenbelt) of 283 air pollution monitoring stations of the MEK in South Korea. The 13 AVHRR types were given at a 1km x 1km pixel resolution (e.g., De Fries et al., 1998; Hansen et al., 2000).

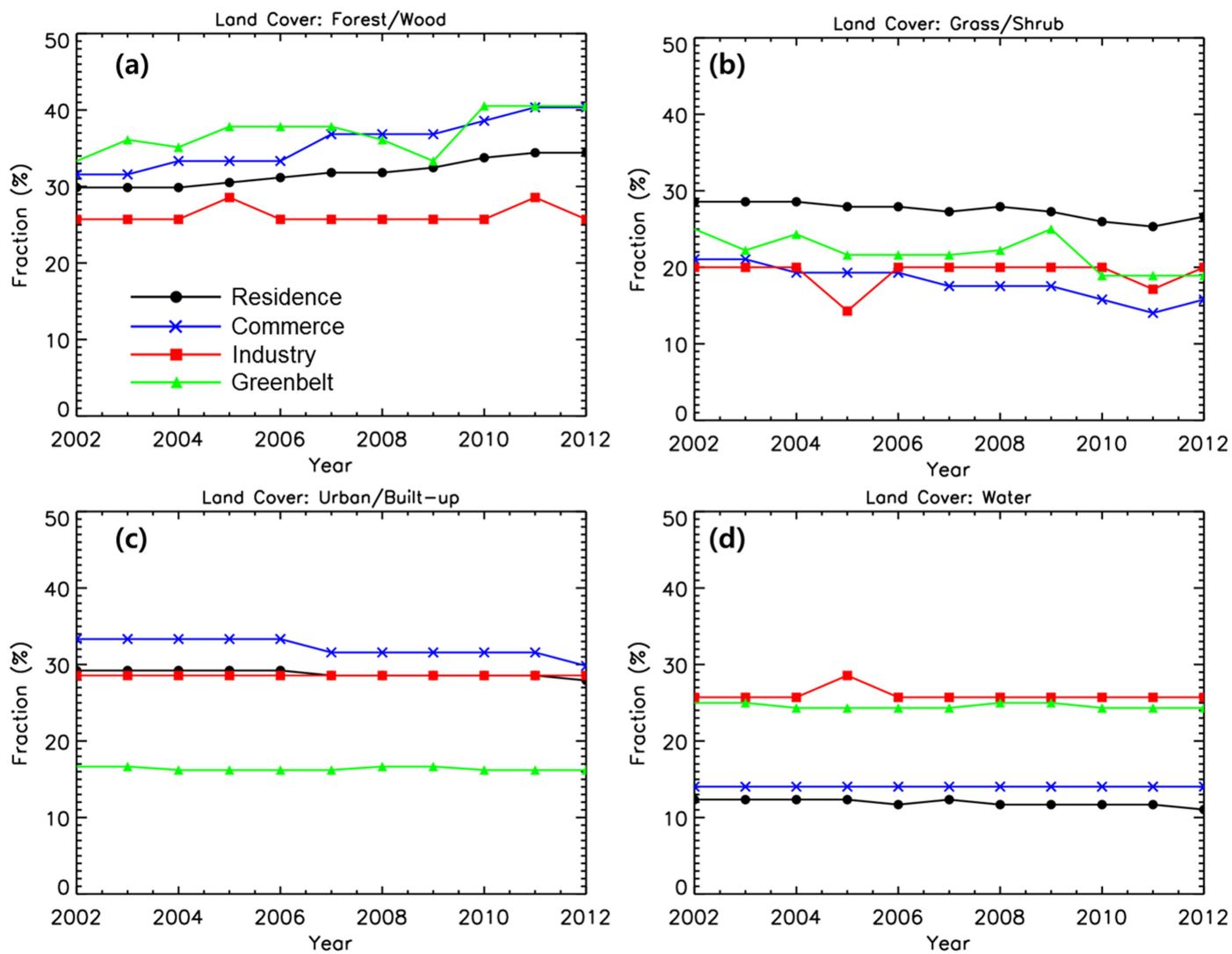


Fig. 3. Interannual variations of the satellite-derived MODIS land-cover types (%) versus the MEK four land-use types (residence, commerce, industry and greenbelt) of the 283 air pollution monitoring stations in South Korea during 2002-2012. In this study, for ease of comparison, the MODIS original types were regrouped into the following four covers; forest/wood, green/shrub, urban/built-up and water.

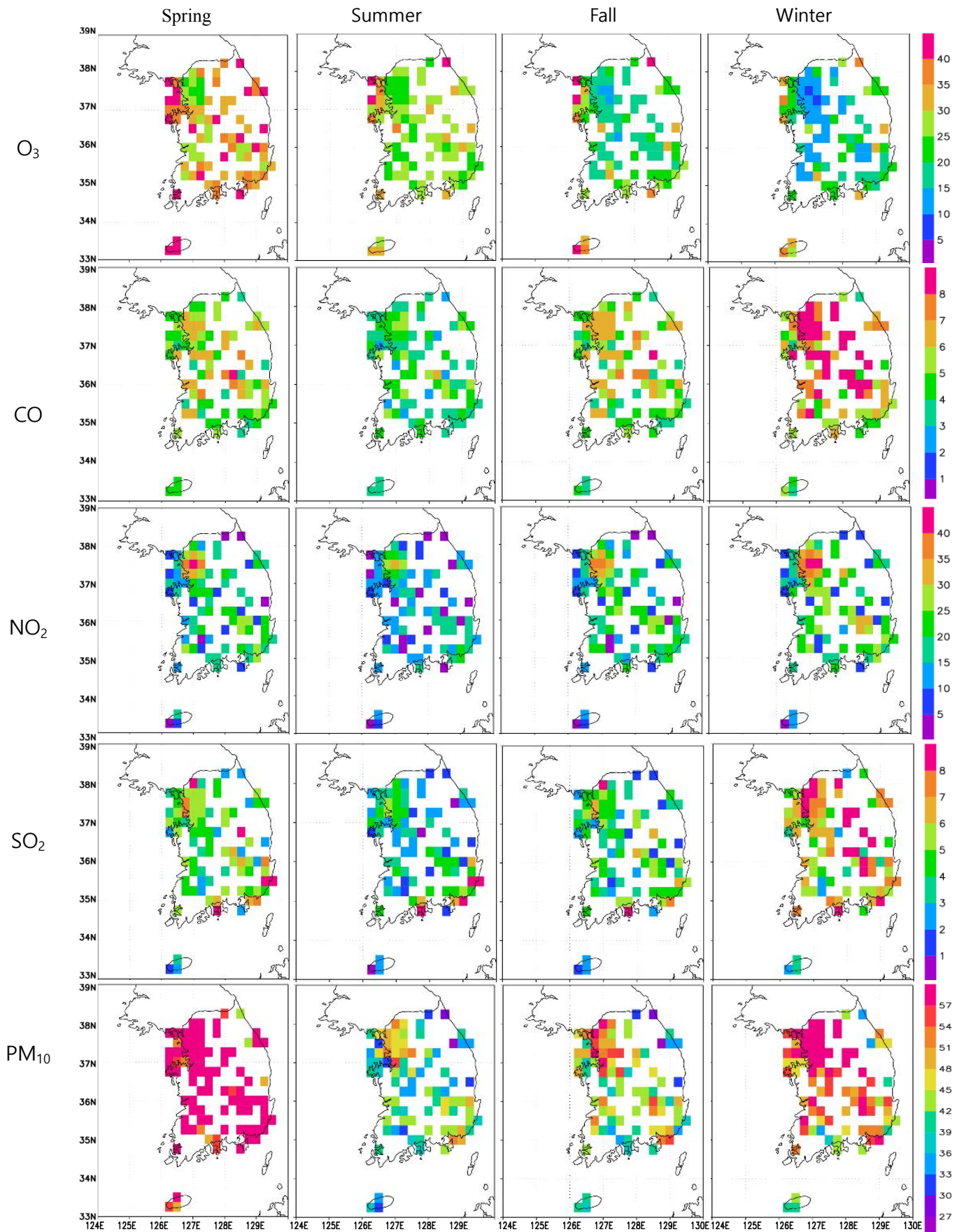


Fig. 4. Climatological seasonal averages of O<sub>3</sub> (ppb), CO (0.1 ppm), SO<sub>2</sub> (ppb), NO<sub>2</sub> (ppb), and PM<sub>10</sub> (μgm<sup>-3</sup>) in a 0.25° x 0.25° grid over South Korea during 2002-2013.

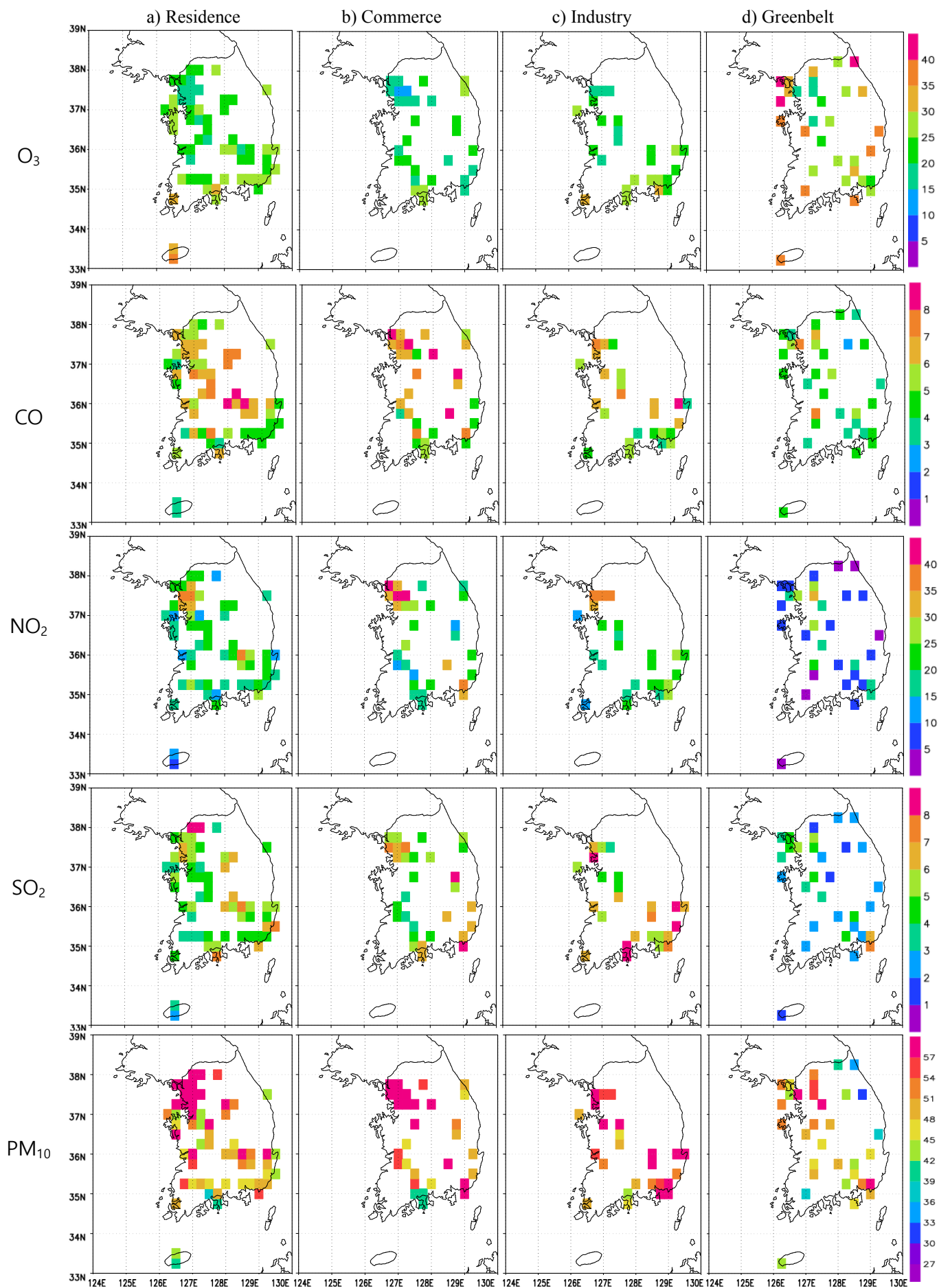


Fig. 5. Climatological annual averages in a  $0.25^{\circ} \times 0.25^{\circ}$  grid over South Korea during 2002-2013 of the surface air pollutant observations of  $O_3$  (ppb), CO (0.1ppm),  $NO_2$  (ppb),  $SO_2$  (ppb), and  $PM_{10}$  ( $\mu g\ m^{-3}$ ) under the MEK four land-use types of a) residence, b) commerce, c) industry, and d) greenbelt.

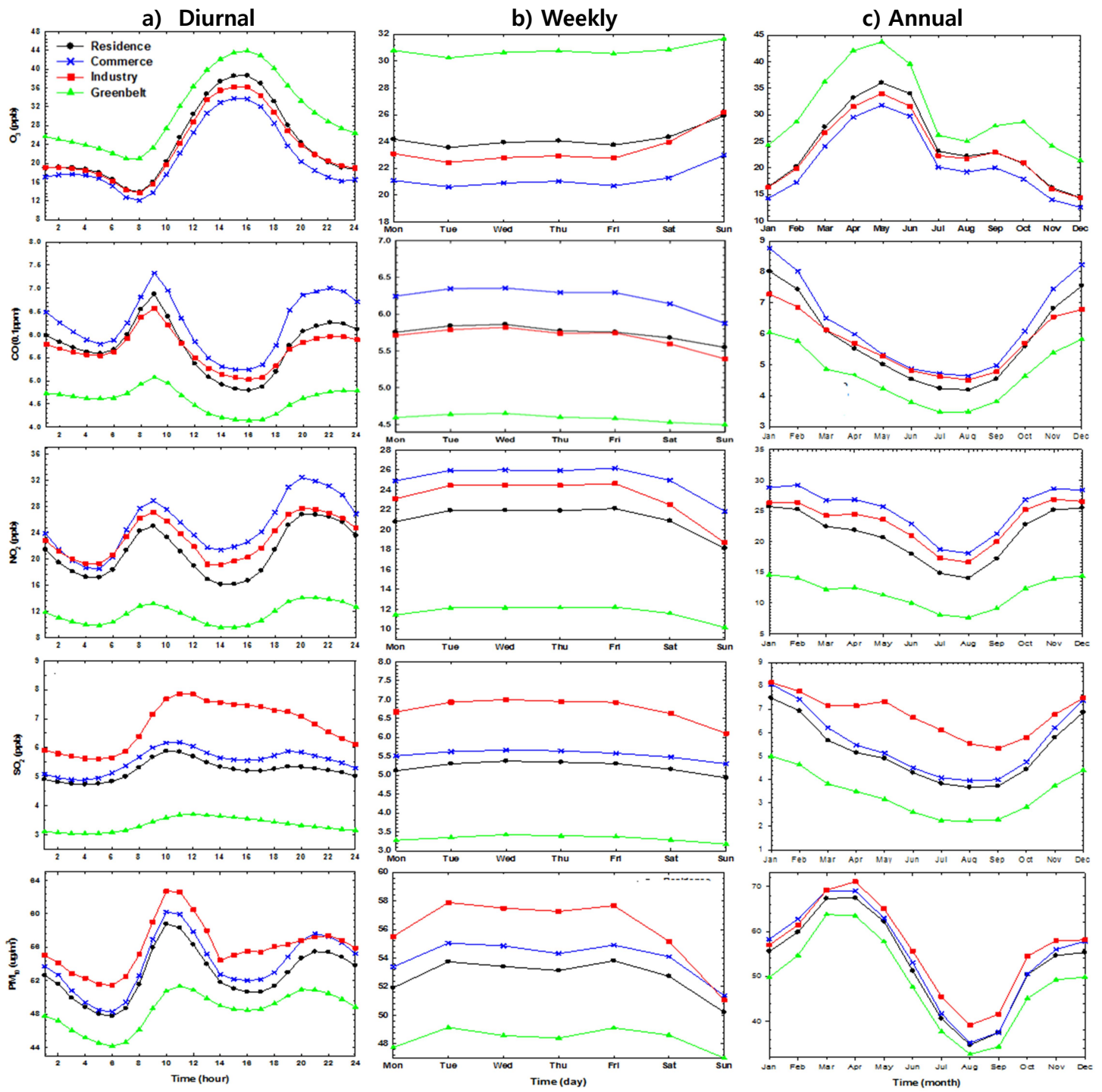


Fig. 6. The (a) diurnal, (b) weekly, and (c) annual variations in a  $0.25^{\circ} \times 0.25^{\circ}$  grid of the O<sub>3</sub> (ppb), CO (0.1ppm), NO (ppb), SO<sub>2</sub>, (ppb) and PM<sub>10</sub> ( $\mu\text{g m}^{-3}$ ) observations over South Korea during 2002-2013 under the MEK four land-use types as follows: residence (black circle), commerce (blue cross), industry (red square) and greenbelt (green triangle).



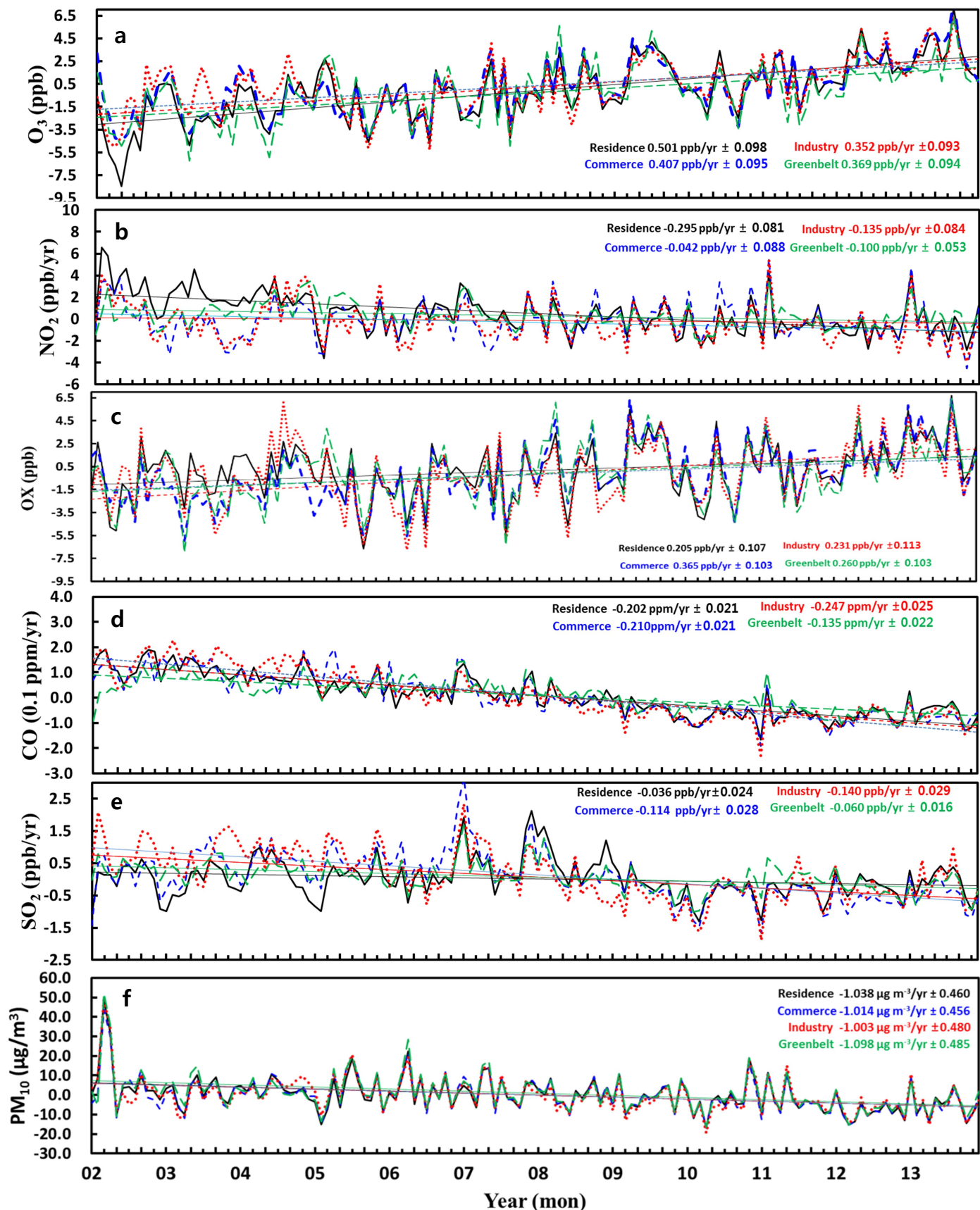


Fig. 7. Time series of the monthly surface air pollutant anomalies in a  $0.25^{\circ} \times 0.25^{\circ}$  grid of the (a) O<sub>3</sub> (ppb), (b) NO<sub>2</sub> (ppb) (c) OX (ppb), (d) CO (0.1 ppm), (e) SO<sub>2</sub> (ppb), and (f) PM<sub>10</sub> ( $\mu\text{g m}^{-3}$ ) observations over South Korea during the period from January 2002 to December 2013 under the following MEK land-use types; residence (black solid), commerce (blue dashed), industry (red dotted) and greenbelt (green dashed). The  $\pm$  trend values define the 95% confidence intervals

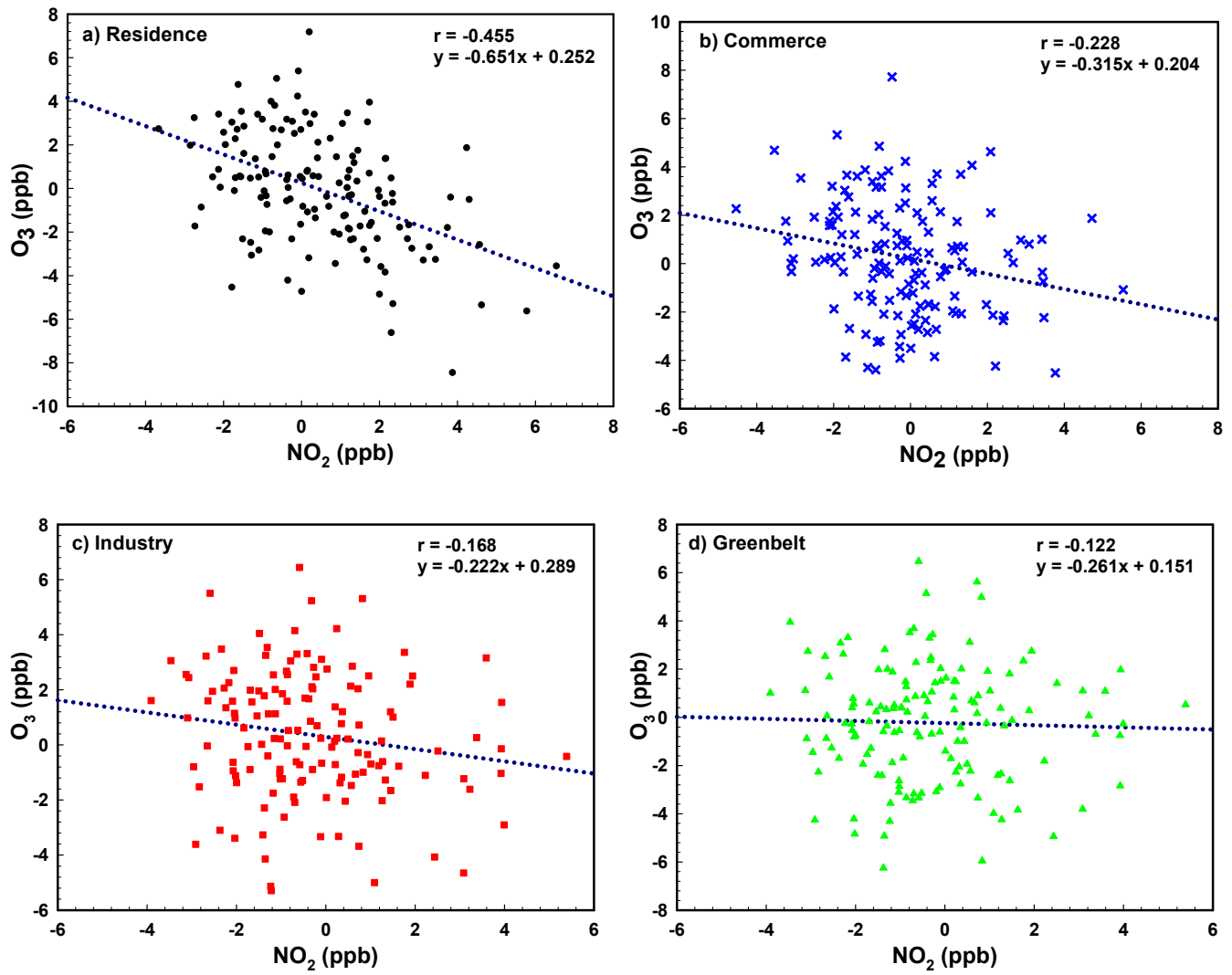


Fig. 8. Scatter diagrams of the monthly anomalies of  $\text{O}_3$  (ppb) versus  $\text{NO}_2$  (ppb) in South Korea during the period from January 2002 to December 2013 under the four land-use types; a) residence (black circle), b) commerce (blue cross), c) industry (red square), and d) greenbelt (green triangle). The correlation coefficient ( $r$ ) and the regression dotted line are also given.

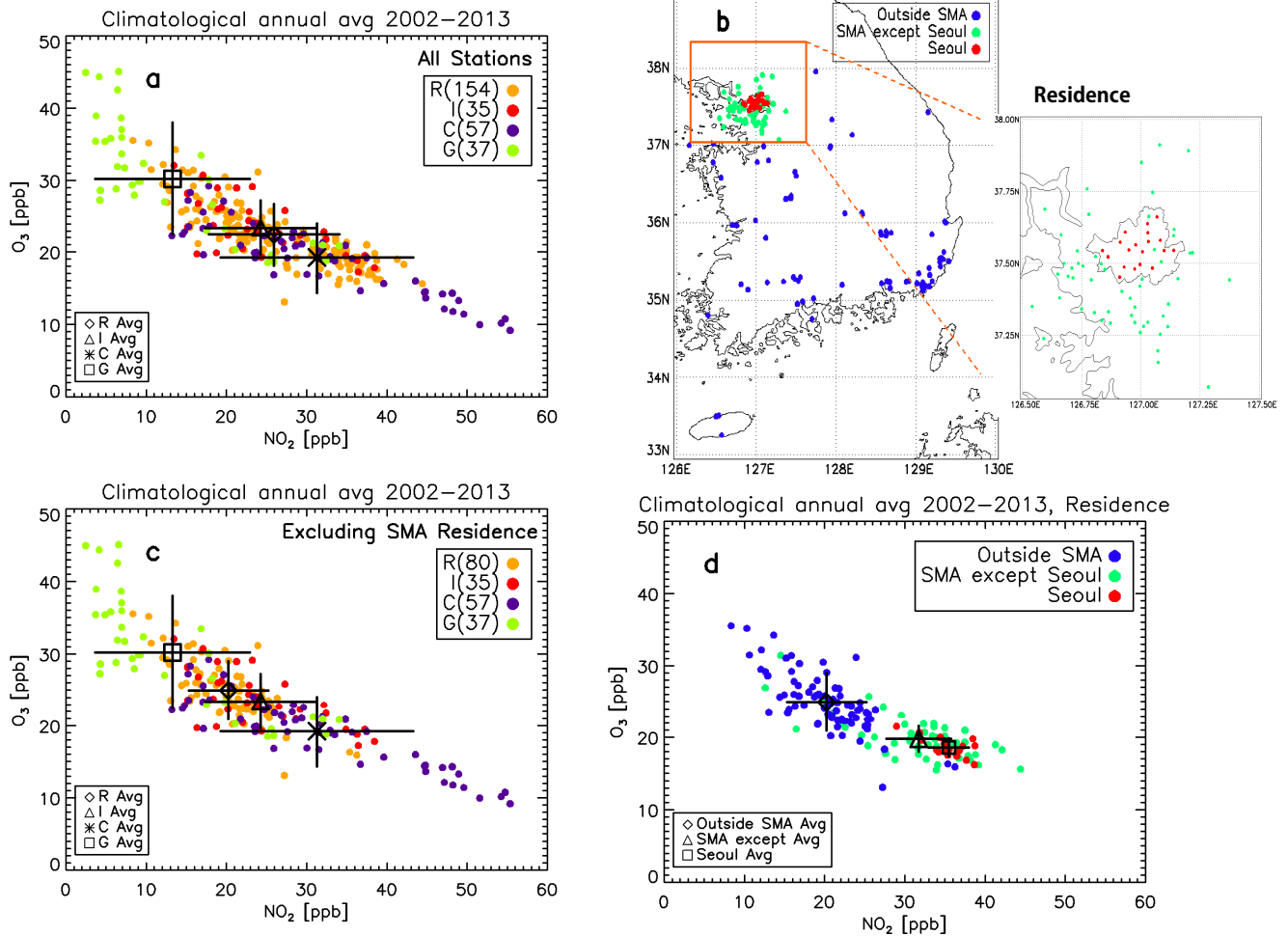


Fig. 9. Climatological annual averages of the  $O_3$  (ppb) versus  $NO_2$  (ppb) over South Korea during 2002-2013 under the MEK four land-use types of residence (R), commerce (C), industry (I), and greenbelt (G). a)  $O_3$  versus  $NO_2$  at whole 283 stations in South Korea. The number in the upper-right side panel of the figure indicates the count of stations. b) Locations of 154 'residence-type' stations subdivided by the three regions as follows; i) Seoul (red circle), ii) the Seoul Metropolitan Area (SMA; green circle) except for Seoul, and iii) outside of the SMA (blue circle). The rectangular area in Fig. 9b indicates that the SMA has been enlarged on the right side. c) Same as Fig. 9a except for excluding the  $O_3$  and  $NO_2$  observations of the SMA residential region. d) Same as Fig. 9a except for using the  $O_3$  and  $NO_2$  only in the 'residence' type under the three different regions of Fig. 9b. The mean values and standard deviations for the annual values of  $NO_2$  and  $O_3$  in each of the types are indicated in Figs. 9a, b, and d.

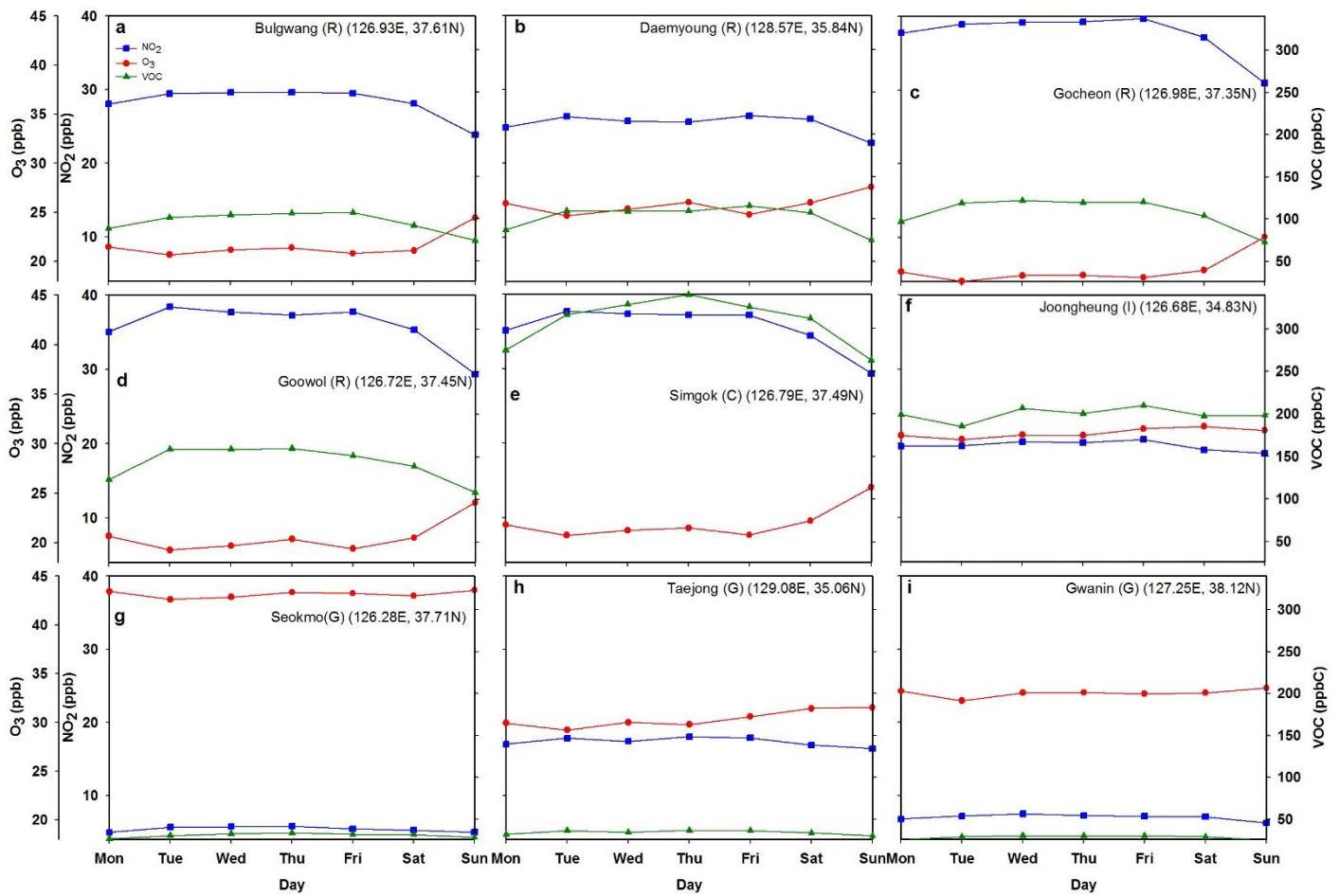


Fig. 10. The weekly variations in the VOCs (green triangle), O<sub>3</sub> (red circle), and NO<sub>2</sub> (blue rectangle) concentrations at the 9 photochemical air pollution monitoring stations in South Korea since 2007 under the MEK four land-use types as follows; residence (R), commerce (C), industry (I), and greenbelt (G). Please see Table 1 for the observational period at each of the VOCs station. For convenience, the terminology of ‘VOC’ in the figures means ‘VOCs’ in the text.

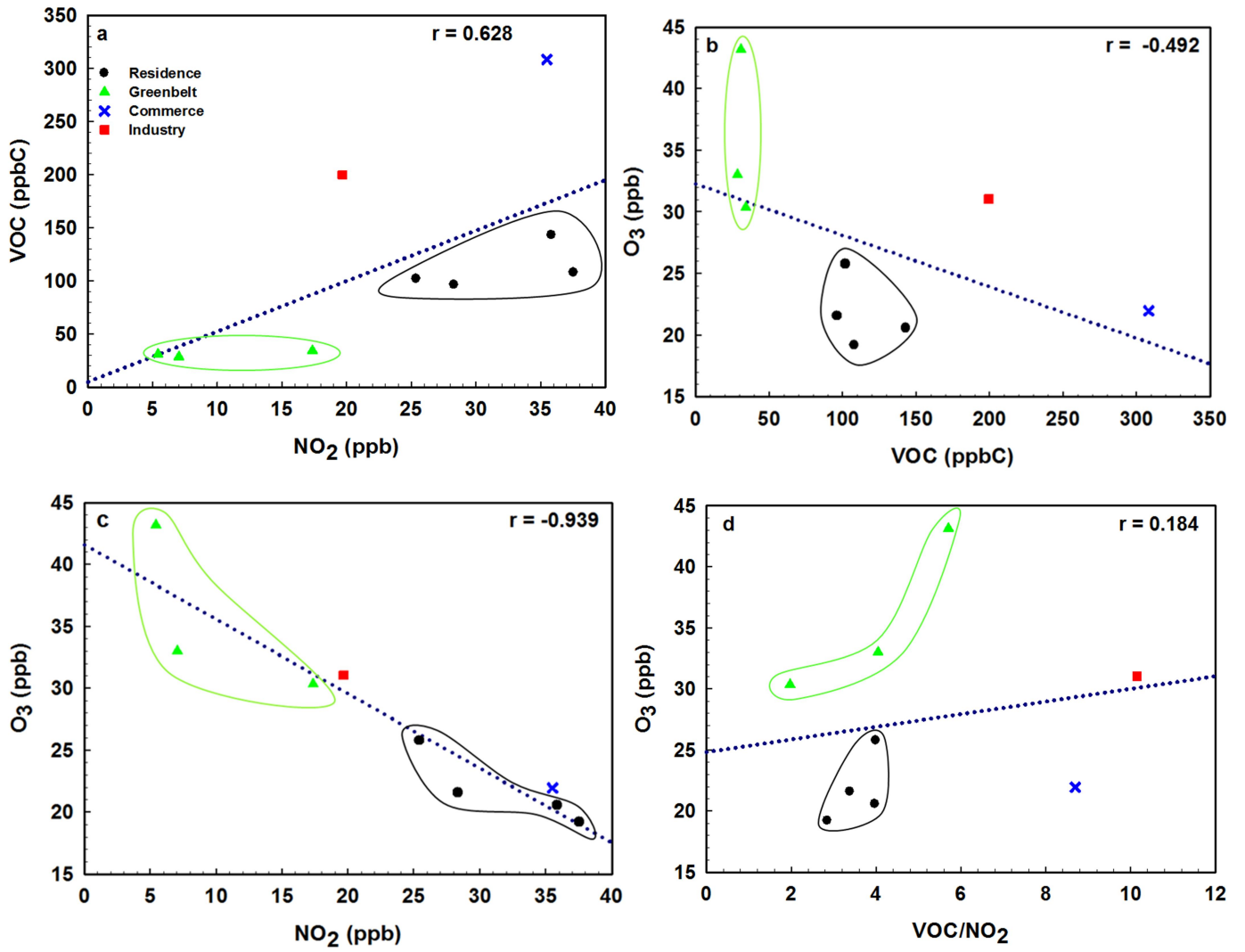


Fig. 11. Scatter diagrams of the long-term averages of a) VOCs versus  $\text{NO}_2$ , b)  $\text{O}_3$  versus VOCs, c)  $\text{O}_3$  versus  $\text{NO}_2$ , and d)  $\text{O}_3$  versus the ratio of  $\text{VOC}/\text{NO}_2$  at 9 of the photochemical air pollution monitoring stations over South Korea since 2007 under the following four land-use types; residence (black circle), commerce (blue cross), industry (red square), and greenbelt (green triangle). The correlation coefficient ( $r$ ) and the regression dotted line were also given.

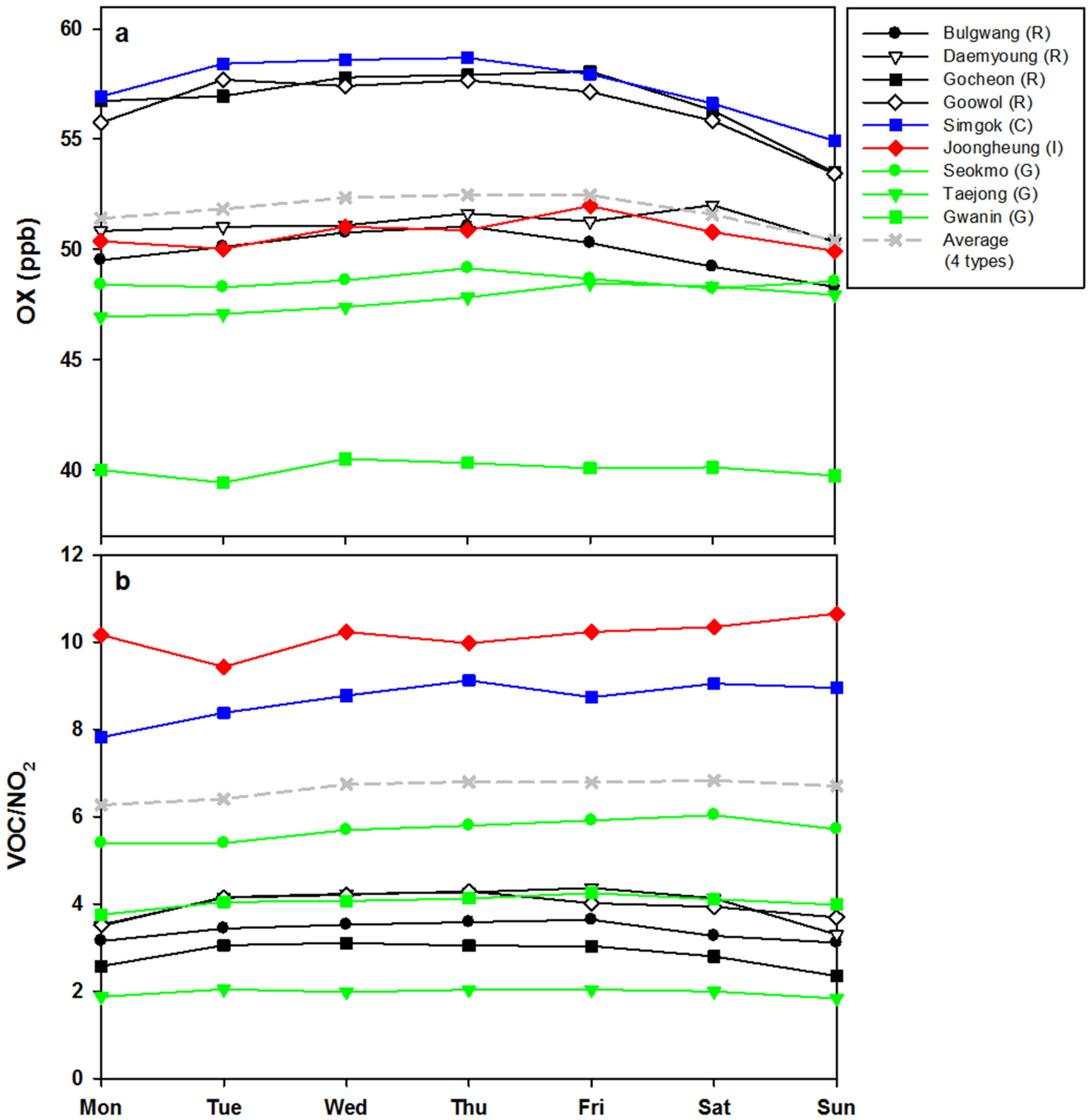


Fig. 12. Weekly variations in the a) OX and b) VOCs/NO<sub>2</sub> values 2007 at nine of the photochemical air pollution monitoring stations of the MEK in South Korea. Please see Table 1 for the observational period at each of the VOCs stations.

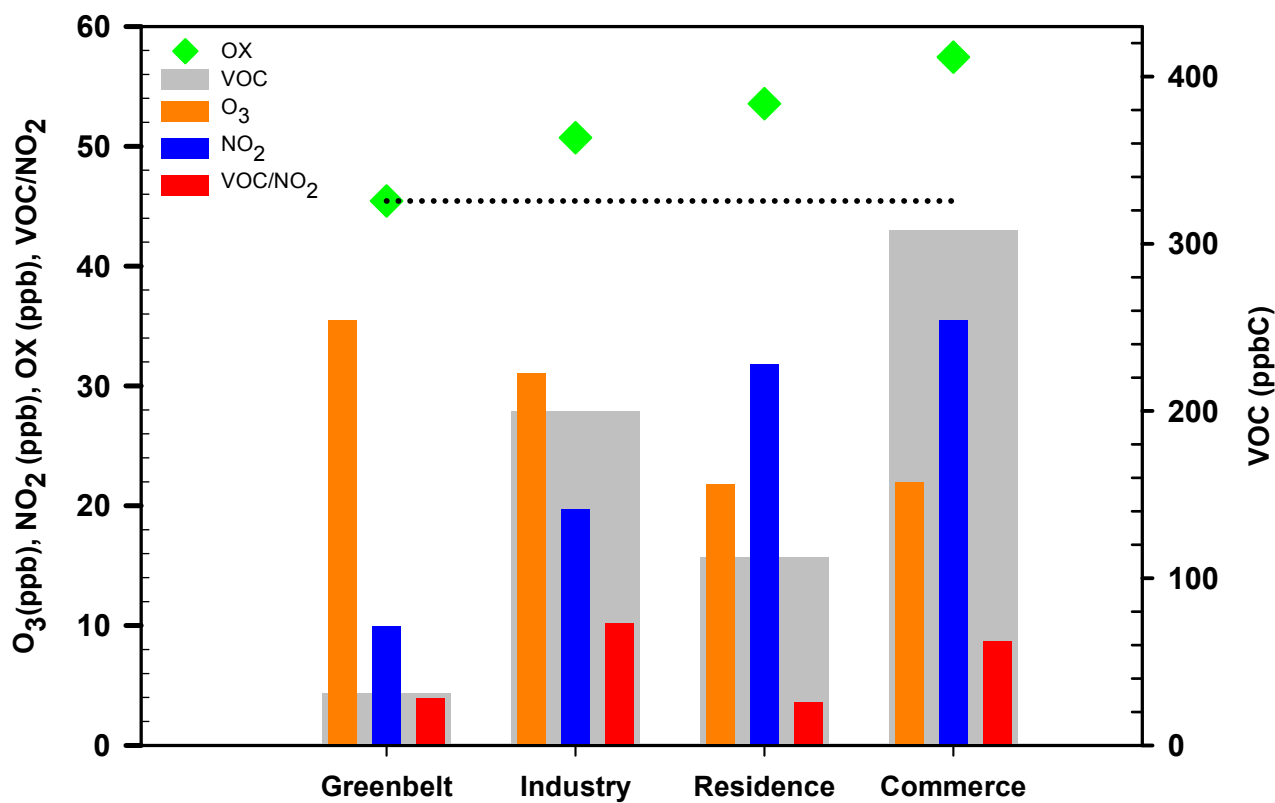


Fig. 13. Climatological averages of the OX (ppb), VOCs (ppbC), O<sub>3</sub> (ppb), NO<sub>2</sub> (ppb) and the ratio of VOCs/NO<sub>2</sub>. The values of the VOCs, O<sub>3</sub>, NO<sub>2</sub>, and the ratio in the bar graph are shown in the colors of grey, salet, blue and red, respectively, at 9 of the photochemical air pollution monitoring stations over South Korea since 2007 under the following MEK four land-use types of residence, commerce, industry, and greenbelt. The OX values are presented as green diamonds. Please see Table 1 for the observational period at each of the VOCs station.